

---

# Value-Guided Decision Transformer: A Unified Reinforcement Learning Framework for Online and Offline Settings

---

Hongling Zheng<sup>1</sup> Li Shen<sup>2†</sup> Yong Luo<sup>1†</sup> Deheng Ye<sup>3</sup> Shuhan Xu<sup>1</sup> Bo Du<sup>1</sup>  
Jialie Shen<sup>4</sup> Dacheng Tao<sup>5</sup>

<sup>1</sup> School of Computer Science, National Engineering Research Center of Multimedia Software and Hubei Key Laboratory of Multimedia and Network Communication Engineering, Wuhan University, Wuhan, China

<sup>2</sup> Shenzhen Campus of Sun Yat-sen University, Shenzhen, China <sup>3</sup> Tencent Inc., Shenzhen, China

<sup>4</sup> City St George's, University of London, UK <sup>5</sup> Nanyang Technological University, Singapore  
{hlzheng, luoyong, xushuhan, dubo}@whu.edu.cn dericye@tencent.com  
{mathshenli, dacheng.tao}@gmail.com jerry.shen@citystgeorges.ac.uk

## Abstract

The Conditional Sequence Modeling (CSM) paradigm, benefiting from the transformer’s powerful distribution modeling capabilities, has demonstrated considerable promise in Reinforcement Learning (RL) tasks. However, much of the work has focused on applying CSM to single online or offline settings, with the general architecture rarely explored. Additionally, existing methods primarily focus on deterministic trajectory modeling, overlooking the randomness of state transitions and the diversity of future trajectory distributions. Fortunately, value-based methods offer a viable solution for CSM, further bridging the potential gap between offline and online RL. In this paper, we propose Value-Guided Decision Transformer (VDT), which leverages value functions to perform advantage-weighting and behavior regularization on the Decision Transformer (DT), guiding the policy toward upper-bound optimal decisions during the offline training phase. In the online tuning phase, VDT further integrates value-based policy improvement with behavior cloning under the CSM architecture through limited interaction and data collection, achieving performance improvement within minimal timesteps. The predictive capability of value functions for future returns is also incorporated into the sampling process. Our method achieves competitive performance on various standard RL benchmarks, providing a feasible solution for developing CSM architectures in general scenarios. Code is available at [here](#).

## 1 Introduction

Offline reinforcement learning (Offline RL) [1] aims to develop a reward-maximizing RL strategy using offline data. This approach is highly valuable in real-world scenarios where online data collection is expensive, time-consuming, or impractical. Transformer [2] is widely regarded for its capacity to capture complex data distributions and long-term temporal dependencies, becoming a foundational architecture in fields such as Natural Language Processing [3, 4] and Computer Vision [5, 6]. Inspired by this success, Decision Transformer (DT) [7] and its variants [8, 9] introduce the transformer to the field of offline RL, demonstrating its powerful capabilities in Conditional Sequence Modeling (CSM) [10]. Specifically, DT integrates cumulative rewards, states, and actions

---

<sup>†</sup>Corresponding authors.

into a tuple and trains on offline datasets autoregressively to output appropriate actions. This approach relaxes the MDP assumption by considering multiple historical steps, allowing the model to handle long sequences and avoid stability issues associated with bootstrapping [11].

The CSM method is essentially goal-conditioned behavior cloning, which optimistically treats the highly incidental performance gains resulting from the randomness in offline data as a general expectation. As a result, while it performs well in deterministic environments, it struggles to achieve good performance in stochastic environments or when faced with suboptimal data. Some works [12, 13] have combined value functions trained on offline data with CSM to generate suboptimal trajectory stitching, guiding the agent’s robust learning. However, these approaches typically introduce the value function by simply re-labeling the return-to-go (RTG) or directly using it as penalty terms, with little consideration given to how to explore further the optimization upper bound of the value function in the CSM setting and effectively integrate it with the DT to curb its overly optimistic behavior cloning.

Bridging the gap between offline and online reinforcement learning remains a central challenge. One promising direction that has emerged in recent years is offline-to-online RL [14, 15]. Within the CSM framework, a commonly used method is the Online Decision Transformer (ODT) [16], which extends DT training into the online phase while maintaining the same supervised learning paradigm used in offline RL. However, ODT faces challenges in achieving expert-level performance in online scenarios with limited or suboptimal data, primarily due to its inability to compose or integrate suboptimal trajectories effectively. Furthermore, ODT demonstrates significant advantages only after online fine-tuning, while its performance in offline scenarios remains suboptimal. There is still limited research on how the CSM architecture can generalize across offline and online settings.

To remedy these drawbacks, we propose the Value-Guided Decision Transformer (VDT), a unified RL framework for online and offline settings. (1) **Offline Training Phase:** Based on the DT training framework, we combine a multi-step Bellman-optimized Q-function and state-value function to explore the upper bound of value estimation. Value guidance is integrated with the behavior cloning of Decision Transformer (DT) through advantage-weighted learning, while the maximum estimated value is concurrently used as a penalty term to regularize the expected value of the current action distribution. The coupling and regularization effectively mitigate the overly optimistic estimates of CSM in stochastic environments and enable trajectory stitching from suboptimal data. (2) **Online Tuning Phase:** VDT refines the value function and the policy through limited interactions. Integrating the trajectory-level replay buffer and RTG alignment achieves significant performance improvements within minimal timesteps. (3) **Sampling Process:** The Q-function evaluates the expected future return of each action the policy generates under different RTGs within a predefined evaluation horizon and selects the optimal decision. The introduction of the value function significantly improves the DT’s performance in both pure offline and offline-to-online settings, regardless of data quality or reward sparsity, and further bridges the potential gap between offline and online RL.

The main contributions of this work are as follows:

- We incorporate the value function into the CSM architecture and enhance behavior cloning with advantage-weighted learning and regularization constraints. These components enable VDT to stitch together suboptimal trajectories under value-based guidance and achieve robust performance across varying-quality datasets. We further provide a theoretical guarantee of its superior performance.
- We leverage the inherent strengths of the value function to fine-tune the policy with a limited number of interactions in the online phase. By introducing the trajectory-level replay buffer and return-to-go alignment, we bridge the gap between offline training and online tuning, offering insights into the design of generalizable architectures.
- We demonstrate the effectiveness of VDT across a broad spectrum of benchmarks, exhibiting superior performance in pure offline and offline-to-online settings.

## 2 Related works

**CSM for Offline RL.** In contrast to online RL, offline RL [17] focuses on training models and performing trial-and-error using offline data without environmental interaction to arrive at appropriate strategies. Recently, CSM for RL [18, 19], represented by the transformer architecture, has further

demonstrated the advantages of data-driven policy learning. DT [7] is trained on an offline dataset of triplets encapsulating return-to-go  $\hat{r}_t$ , state  $s_t$ , and action  $a_t$ , and outputs the optimal action. The  $\hat{r}_t$  token quantifies the cumulative reward from the current time step to the end of the episode. During training, DT processes a trajectory sequence  $\tau_t$  in an auto-regressive manner, which encompasses the most recent  $K$ -step historical context:

$$\tau_t = (\hat{r}_{t-K+1}, s_{t-K+1}, a_{t-K+1}, \dots, \hat{r}_t, s_t, a_t) \quad (1)$$

The prediction head associated with a state token  $s_t$  is trained to predict the corresponding action  $a_t$ . Regarding continuous action spaces, the training objective is to minimize the mean-squared loss  $L_{DT}$ .

$$L_{DT} = \mathbb{E}_{\tau_t \sim \mathcal{D}} \left[ \frac{1}{K} \sum_{t=t-K+1}^K (a_t - \pi_\theta(\tau_t)_i)^2 \right] \quad (2)$$

Subsequent work has made various improvements to DT, including prompt tuning [20], trajectory concatenation [21], and value regularization [22]. These approaches often involve more complex modifications of DT to adapt it to specific tasks.

**Offline-to-Online RL.** Offline-to-online RL focuses on fine-tuning a policy pre-trained on offline data using a limited number of online interactions to improve performance and narrow the gap between offline and online learning. Key challenges in this setting include effectively leveraging offline data for initializing the policy and mitigating distributional shifts during the online adaptation process. Early approaches focus on pre-training policies with offline data [23, 24] and use techniques such as balanced sampling [25], adaptive conservatism [15], and actor-critic alignment [26] to stabilize the transition to the online phase. For efficient online fine-tuning, optimistic exploration strategies are employed, utilizing Q-ensembles [27], uncertainty-guided exploration [28], or model-based uncertainty estimation [29]. While most existing methods follow Q-learning paradigms, the use of CSM architectures such as DT for offline-to-online reinforcement learning remains largely underexplored.

**Value-based Offline RL.** The value-based method is one of the most prominent categories for addressing the distribution shift problem in offline RL. Primarily previous works generally address this problem in one of three ways: (1) constraining the learned policy to the behavior policy [23, 30]; (2) constraining the learned policy by making conservative estimates of future rewards [24, 22]; (3) introducing model-based methods, which learn a model of the environment dynamics to generate more data for policy training and perform pessimistic planning in the learned MDP [31, 32].

The most relevant work to ours is ODT [16], the first to establish a pipeline for transitioning from offline to online RL within the DT framework. However, since ODT adopts a strategy that mirrors its offline training phase, it struggles to effectively handle suboptimal data and adapt to dynamic or stochastic environments. Moreover, as a few-shot method primarily focused on online fine-tuning, ODT performs significantly worse than most baselines in offline settings. TD3+ODT [33], which is primarily based on the ODT algorithm pipeline, further incorporates the RL gradient from the critic as an additional penalty term in the loss function. Our method is distinguished by the effective optimization of the value function and its integration with the DT, enabling the policy to achieve robust performance across varying data quality in offline and online settings. In addition, the evaluation mechanism we design during the sampling process further encourages exploration, facilitating efficient trajectory stitching.

### 3 Preliminary

**Markov Decision Process.** Reinforcement Learning is typically formulated as a Markov Decision Process (MDP), defined by a tuple  $(\mathcal{S}, \mathcal{A}, P, r, \gamma)$ , where  $\mathcal{S}$  represents the state space,  $\mathcal{A}$  is the action space,  $P$  is the transition function,  $r$  is the reward function, and  $\gamma \in [0, 1]$  is the discount factor.

In offline RL, the objective is to optimize the RL policy using a previously collected dataset  $D = \{(s_t^i, a_t^i, r_t^i, s_{t+1}^i)\}_{i=0}^{N-1}$ , consisting of  $N$  trajectories. The key distinction in offline RL is that the agent does not interact directly with the environment during the learning phase but instead learns from the historical data. This offline dataset represents the state-action-reward-state transitions the agent experienced during earlier episodes. The agent’s task is to extract useful information from these trajectories to improve its decision-making policy without further environmental exploration.

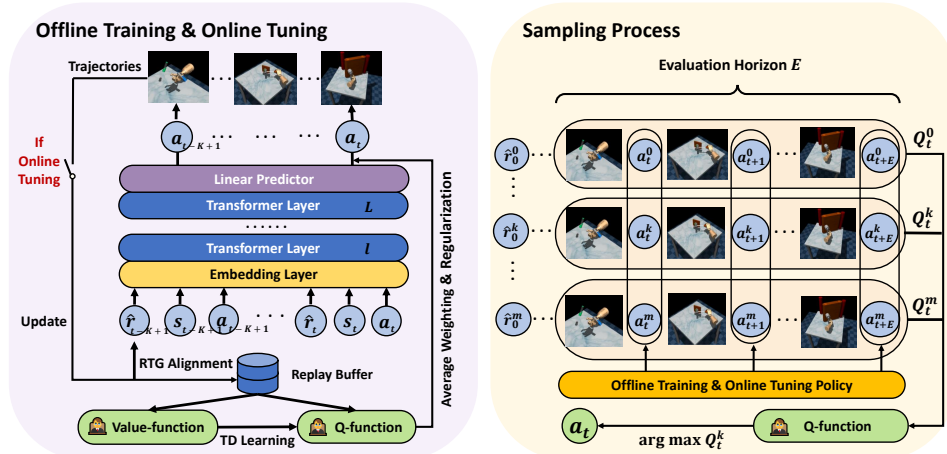


Figure 1: The architecture of Value-Guided Decision Transformer. **Left: Offline Training & Online Tuning.** VDT is trained offline under value guidance and interacts with the environment online to generate trajectories for updating the replay buffer. These trajectories are then used to tune VDT further. **Right: Sampling Process.** At a specific timestep  $t$ , the policy generates candidate actions within the evaluation horizon  $E$  under predefined RTGs, and evaluates them using the Q-function to obtain the optimal action  $a_t$ .

**Online Decision Transformer.** Online Decision Transformer (ODT) operates in two stages: *offline pretraining* and *online finetuning*. In the offline phase, the model learns from static trajectories using supervised learning, following the standard DT paradigm. In the online phase, it collects new trajectories and refines the policy with supervised updates. During rollouts, the action  $a_t$  at timestep  $t$  is either computed deterministically as  $a_t = \mu_{\text{DT}}(\tau_t)$ , or sampled stochastically from the policy  $a_t \sim \pi_{\text{DT}}(a_t | \tau_t)$ . The policy is initialized using the offline dataset and is updated during finetuning as newly collected online trajectories gradually replace the old data buffer.

## 4 Method

This section provides a comprehensive description of the proposed VDT. We break down VDT into three parts: offline training, online tuning, and the sampling process. The **offline training** details how the value function is integrated into the conventional CSM architecture using advantage-weighted learning and regularization terms. The **online tuning** focuses on the collection and processing of online data. Although the model has already incorporated the value guidance during training, due to the inherent randomness of the environment, we perform value evaluation on the predicted actions during the **sampling process** to maximize decision-making performance.

### 4.1 Offline Training

We incorporate value guidance into the DT architecture to enable the CSM architecture to perform robustly in highly stochastic environments and with suboptimal trajectories, and to achieve effective trajectory stitching. As a first step, we learn the Q-function. Specifically, we aim to estimate an upper bound of the Q-function within the support of the dataset’s action distribution. We implement the Q-networks  $Q_{\theta_1}(s, a)$  and  $Q_{\theta_2}(s, a)$ , along with their corresponding target networks  $Q_{\hat{\theta}_1}(s, a)$  and  $Q_{\hat{\theta}_2}(s, a)$ , as multi-layer perceptrons (MLPs) with two hidden layers. This architecture provides sufficient representational capacity to approximate complex value functions while maintaining stability during offline training. Inspired by Implicit Q-Learning (IQL) [24], we adopt an expectancy regression technique, which leverages an asymmetric L2 loss to provide an unbiased estimation of the conditional expectile. For a given threshold  $\epsilon > 0.5$ , this loss function adaptively emphasizes high-return actions by down-weighting the influence of actions with returns below the threshold, thereby approximating the conditional upper bound of the Q-function. To support this, we use an independent state-value function  $V_{\phi}(s)$ , implemented as a simple two-layer MLP, and optimize it

using the following objective:

$$L_V(\psi) = \mathbb{E}_{(s_t, a_t) \sim \mathcal{D}} [L_2^\epsilon(Q_{\hat{\theta}}(s_t, a_t) - V_\psi(s_t))], \quad (3)$$

where  $L_2^\epsilon(u) = |\epsilon - \mathbb{I}(u < 0)|u^2$ . After obtaining the  $V_\psi$  with average properties, given that the input to the DT consists of historical trajectories, we choose the n-step Bellman equation to estimate the double Q-networks, which has been shown to provide better stability in practical training compared to single-step optimization [34]. To update  $Q_{\theta_i}, i \in [1, 2]$ , we use the following formula:

$$\mathbb{E}_{(s_t, a_t, r_t, \dots, s_{t+n}) \sim \mathcal{D}} \left[ \left( \sum_{k=0}^{n-1} \gamma^k r_{t+k} + \gamma^n V_\psi(s_{t+n}) - Q_{\theta_i}(s_t, a_t) \right)^2 \right] \quad (4)$$

where  $\gamma$  is the discount factor. We modify the TD learning procedure to learn an approximation to the optimal Q-function on an offline dataset. In designing the learning objective, we weigh the DT’s trajectory modeling loss by computing the advantage function  $\min_{i=1,2} Q_{\hat{\theta}_i}(s_t, a_t) - V_\psi(s_t)$ , which helps the model identify high-return action trajectories in the dataset and assign them higher importance. As proposed by [35], this advantage-weighted method performs policy optimization within the action distribution supported by the dataset, stabilizing the learning process. Additionally, to further guide the policy towards high-value directions, we compute the policy’s action output at the current state and evaluate its value using the target Q-networks, which is then incorporated into the loss function as a regularization term.

$$\mathbb{E}_{\substack{\tau_t \sim \mathcal{D} \\ (s_t, a_t) \sim \tau_t}} [\exp(\eta(\min_{i=1,2} Q_{\hat{\theta}_i}(s_t, a_t) - V_\psi(s_t))) \|\pi_{DT}(\tau_t) - a_t\|^2 - \lambda \cdot \min_{i=1,2} Q_{\hat{\theta}_i}(s_t, \pi_{DT}(\tau_t))] \quad (5)$$

where  $\eta$  is an inverse temperature, which we set to 3. The parameter  $\lambda$  is a hyperparameter that balances the weight between the two loss terms. Through this loss design, the combination of advantage weighting and the regularization term optimizes the stability of trajectory modeling while guiding the value function to break through the local optima within the data distribution.

**Theorem 4.1.** *Let  $\pi_{DT}^*$  be the optimal policy of Equation 5. For any  $s \in S$ , we have that  $V^{\pi_{DT}^*}(s) \geq V^\beta(s)$  and  $\pi^*(\mathbf{a} | s) = 0$  given  $\beta(\mathbf{a} | s) = 0$ .*

**Theorem 4.2.** *For any initial state distribution  $\mu$ , we have that  $V^{\pi^*}(\mu) - V^{\pi_{DT}^*}(\mu) \leq \frac{2\gamma}{(1-\gamma)^2} \cdot \mathbb{E}_{s \sim d^{\pi^*}} [\max_{a \notin \mathcal{A}_D(s)} Q^{\pi^*}(s, a) - \max_{a \in \text{supp}(\beta(\cdot|s))} Q^{\pi^*}(s, a)]$ .*

Building on the theoretical foundations established by Theorem 4.1 and the new upper bound provided by Theorem 4.2, we further confirm the effectiveness of Equation 5. These theoretical insights suggest that a policy guided by the value function is likely to outperform the behavior policy. In particular, advantage-weighting and regularization play a crucial role by prioritizing high-value actions, thus steering the learning process towards optimal returns and ensuring consistent improvement over the baseline behavior policy  $\beta$ . Complete proofs are provided in Appendix A and Appendix B.

## 4.2 Online Tuning

During the online tuning stage, while following almost the same pipeline as the offline training phase, we also introduce several distinct components to achieve the most significant performance gains with the fewest interaction steps.

**Trajectory-Level Replay Buffer.** In the online tuning phase, we employ a replay buffer similar to that used in ODT [16], where the buffer consists of entire trajectories rather than individual transitions. The replay buffer is initially populated with the trajectories that yield the highest returns in the offline dataset. Each time the policy interacts with the environment, we fully roll out an episode using the current policy, then refresh the replay buffer by adding the collected trajectory in a first-in-first-out manner. Afterwards, we update the policy and proceed with another rollout. We use the two-step sampling procedure to ensure that the sub-trajectories of length  $K$  in the replay buffer  $T_{replay}$  are sampled uniformly. We first sample a single trajectory with probability proportional to its length, then uniformly sample a sub-trajectory of length  $K$ . Our sampling strategy is akin to importance sampling for environments with non-negative, dense rewards. In those cases, the length of a trajectory is highly correlated with its return.

**Return-to-go Alignment.** During the offline training phase, the RTG at the current step is accumulated from subsequent rewards, and the policy learns conditioned on this RTG. However, in the online

tuning phase, the policy interacts with the environment in real-time based on a predefined RTG, and the induced RTG may differ from the predefined RTG. This discrepancy leads to a mismatch between the expected and actual returns, further affecting the effectiveness of the value function in guiding the policy. To address this, we modify the RTG token at each step of the rolled-out trajectory using the achieved returns, such that the RTG token at time step  $t$  is set as  $RTG_t = \sum_{j=t}^{|\tau|} r_j$ , where  $|\tau|$  denotes the trajectory length and  $r_j$  denotes the reward at each step. Specifically, for the last timestep of a trajectory, the RTG token equals the immediate reward obtained by the agent upon trajectory termination, which more accurately reflects the return at that step and helps to align the expected and actual returns. Note that, depending on the properties of the environment, the immediate reward at the final step is not necessarily zero.

### 4.3 Sampling Process

Traditional DT uses multiple RTGs for completely independent evaluations and typically selects the trajectory with the highest cumulative return under a specific RTG as the evaluation result, neglecting the potential guidance from alternative RTGs at each timestep. We incorporate multiple RTGs at each trajectory step to overcome this limitation. The value function evaluates the candidate actions, and the optimal action is chosen as the unified decision across all RTG-guided trajectories at that step. This strategy guarantees a unique evaluation outcome, eliminates manual trajectory selection, and effectively integrates the strengths of all RTGs. Specifically, we predefine  $m$  candidate RTGs  $(\hat{r}_0^0, \hat{r}_0^1, \dots, \hat{r}_0^m)$  and maintain  $m$  parallel trajectories. At each timestep  $t$ , the policy simultaneously generates  $m$  candidate actions  $(a_t^0, a_t^1, \dots, a_t^m)$ , where  $a_t^k$  is generated under the guidance of RTG  $\hat{r}_0^k$ . To evaluate these candidates, we introduce an evaluation horizon  $E$ . For specific candidate action  $a_t^k$ , the model autoregressively predicts the subsequent  $E$ -step trajectory  $\tau_t^k = (s_t, a_t^k, s_{t+1}^k, a_{t+1}^k, \dots, s_{t+E}^k)$  under the corresponding RTG  $\hat{r}_0^k$ , and then computes the cumulative action-value sum over the horizon:

$$Q_t^k = \sum_{i=0}^E \gamma^i \cdot Q(s_{t+i}^k, a_{t+i}^k), \quad (6)$$

where  $Q$  denotes the action-value function and  $\gamma$  is the discount factor. The optimal action  $a_t$  is selected as  $a_t = \arg \max_{a_t^k} Q_t^k$ . This optimal action is then appended to all  $m$  trajectories and used to interact with the environment to obtain the next state and reward shared across the  $m$  parallel trajectories. Crucially, the parallel nature of trajectory prediction across candidates ensures computational efficiency—despite evaluating  $m$  trajectories, the batched computation on modern GPUs results in latency comparable to single-trajectory inference. By employing a value function to evaluate and select the optimal action, we effectively integrate guidance from different RTGs, achieving optimal decision-making at each step while maintaining constant inference time. We concisely outline the VDT pipeline in Appendix D.

Our sampling procedure shares similarities with both CEM [36] and SfBC [37]. Like CEM, we generate multiple candidate actions at each step, evaluate them with a value function over a short planning horizon, and select the best one—essentially a single-step population-based search. Unlike SfBC, which samples from a behavior policy and selects by Q-value, VDT uses RTGs to guide candidate actions and evaluates them in parallel. This integration of RTG guidance and batch evaluation allows VDT to combine the strengths of population search and candidate selection while maintaining efficient inference.

## 5 Experiment

In this section, we extensively evaluate our proposed Value-Guided Decision Transformer (VDT) using the widely recognized D4RL benchmark [38]. As an integrated framework, VDT focuses on performance in offline and offline-to-online (hereafter referred to as "online" for simplicity, without causing ambiguity) settings in the main experiments to ensure the model’s generality. Since the offline and online pipelines are nearly identical, we conduct ablation studies under the offline setting to evaluate the shared components.

**Datasets.** We consider five different domains of tasks in the widely used D4RL benchmark: Gym, Adroit, Kitchen, AntMaze and Maze2D. A detailed introduction to these five environments is presented in Appendix E.

**Baselines.** In the offline training phase, we compare VDT with representative offline RL algorithms from value-based and CSM methods. For value-based methods, including BEAR [39], BCQ [40], CQL [23], MoRel [41], O-RL [42] and COMBO [31]. For CSM methods, including DT, DD [43], EDAC [44], D-QL [45], MPPI [46], StAR [47], GDT [48] and CGDT [12]. In the online tuning phase, we compare VDT with ODT, IQL [24], AWAC [49], CQL [23] and PDT [9], SAC [50] and TD3+BC [51]. The performance scores for these baseline methods are sourced from the best results published in respective papers or from our runs, ensuring a fair comparison.

**Implementation details.** All experiments are carried out on a server with 8 NVIDIA 3090 GPUs, each with 24GB of memory. The experimental hyperparameter configurations of VDT are shown in Appendix C.

## 5.1 Main Experiment

Table 1: Offline training performance of VDT and state-of-the-art baselines on D4RL tasks. For VDT, results are reported as the mean and standard error of normalized rewards over 30 random rollouts (3 independently trained models with 10 trajectories each), generally showing low variance.

| Dataset                      | Value-Based Methods |            |            |             |              | Conditional Sequence Modeling Methods |             |             |             |             |            |                        |
|------------------------------|---------------------|------------|------------|-------------|--------------|---------------------------------------|-------------|-------------|-------------|-------------|------------|------------------------|
| <b>Gym Tasks</b>             | <b>BEAR</b>         | <b>BCQ</b> | <b>CQL</b> | <b>IQL</b>  | <b>MoRel</b> | <b>BC</b>                             | <b>DT</b>   | <b>StAR</b> | <b>GDT</b>  | <b>CGDT</b> | <b>DC</b>  | <b>VDT</b>             |
| halfcheetah-medium-replay-v2 | 38.6                | 34.8       | 37.5       | <b>44.1</b> | 40.2         | 36.6                                  | 36.6        | 36.8        | 40.5        | 40.4        | 41.3       | 39.4 $\pm$ 2.0         |
| hopper-medium-replay-v2      | 33.7                | 31.1       | 95.0       | 92.1        | 93.6         | 18.1                                  | 82.7        | 29.2        | 85.3        | 93.4        | 94.2       | <b>96.0</b> $\pm$ 1.9  |
| walker2d-medium-replay-v2    | 19.2                | 13.7       | 77.2       | 73.7        | 49.8         | 32.3                                  | 79.4        | 39.8        | 77.5        | 78.1        | 76.6       | <b>82.3</b> $\pm$ 2.1  |
| halfcheetah-medium-v2        | 41.7                | 41.5       | 44.0       | <b>47.4</b> | 42.1         | 42.6                                  | 42.6        | 42.9        | 42.9        | 43.0        | 43.0       | 43.9 $\pm$ 0.7         |
| hopper-medium-v2             | 52.1                | 65.1       | 58.5       | 63.8        | 95.4         | 52.9                                  | 67.6        | 59.5        | 77.1        | 96.9        | 92.5       | <b>98.3</b> $\pm$ 0.1  |
| walker2d-medium-v2           | 59.1                | 52.0       | 72.5       | 79.9        | 77.8         | 75.3                                  | 74.0        | 73.8        | 76.5        | 79.1        | 79.2       | <b>81.6</b> $\pm$ 1.7  |
| halfcheetah-medium-expert-v2 | 53.4                | 69.6       | 91.6       | 86.7        | 53.3         | 55.2                                  | 86.8        | 93.7        | 93.2        | 93.6        | 93.0       | <b>93.9</b> $\pm$ 0.1  |
| hopper-medium-expert-v2      | 96.3                | 109.1      | 105.4      | 91.5        | 108.7        | 52.5                                  | 107.6       | 111.1       | 111.1       | 107.6       | 110.4      | <b>111.5</b> $\pm$ 3.8 |
| walker2d-medium-expert-v2    | 40.1                | 67.3       | 108.8      | 109.6       | 95.6         | 107.5                                 | 108.1       | 109.0       | 107.7       | 109.3       | 109.6      | <b>110.4</b> $\pm$ 0.9 |
| Average                      | 48.2                | 53.8       | 77.6       | 76.5        | 72.9         | 52.6                                  | 76.2        | 66.2        | 79.1        | 82.4        | 82.2       | <b>84.1</b>            |
| <b>Adroit Tasks</b>          | <b>BEAR</b>         | <b>BCQ</b> | <b>CQL</b> | <b>IQL</b>  | <b>MoRel</b> | <b>EDAC</b>                           | <b>BC</b>   | <b>DT</b>   | <b>D-QL</b> | <b>StAR</b> | <b>GDT</b> | <b>VDT</b>             |
| pen-human-v1                 | -1.0                | 66.9       | 37.5       | 71.5        | -3.2         | 52.1                                  | 63.9        | 79.5        | 72.8        | 77.9        | 92.5       | <b>126.7</b> $\pm$ 4.3 |
| hammer-human-v1              | 2.7                 | 0.9        | 4.4        | 1.4         | 2.3          | 0.8                                   | 1.2         | 3.7         | 0.2         | 3.7         | <b>5.5</b> | 3.2 $\pm$ 0.3          |
| door-human-v1                | 2.2                 | -0.05      | 9.9        | 4.3         | 2.3          | 10.7                                  | 2.0         | 14.8        | 0.0         | 1.5         | 18.6       | <b>19.7</b> $\pm$ 0.5  |
| pen-cloned-v1                | -0.2                | 50.9       | 39.2       | 37.3        | -0.2         | 68.2                                  | 37.0        | 75.8        | 57.3        | 33.1        | 86.2       | <b>145.6</b> $\pm$ 4.0 |
| hammer-cloned-v1             | 2.3                 | 0.4        | 2.1        | 2.1         | 2.3          | 0.3                                   | 0.6         | 3.0         | 3.1         | 0.3         | 8.9        | <b>19.6</b> $\pm$ 1.6  |
| door-cloned-v1               | 2.3                 | 0.01       | 0.4        | 1.6         | 2.3          | 9.6                                   | 0.0         | 16.3        | 0.0         | 0.0         | 19.8       | <b>30.6</b> $\pm$ 0.7  |
| Average                      | 1.0                 | 19.8       | 15.6       | 19.7        | 1.0          | 23.6                                  | 17.5        | 32.2        | 22.2        | 19.4        | 38.9       | <b>57.6</b>            |
| <b>Kitchen Tasks</b>         | <b>BEAR</b>         | <b>BCQ</b> | <b>CQL</b> | <b>IQL</b>  | <b>O-RL</b>  | <b>BC</b>                             | <b>DT</b>   | <b>DD</b>   | <b>StAR</b> | <b>GDT</b>  | <b>DC</b>  | <b>VDT</b>             |
| kitchen-complete-v0          | 0.0                 | 8.1        | 43.8       | 62.5        | 2.0          | 65.0                                  | 50.8        | 65.0        | 40.8        | 43.8        | 40.9       | <b>65.9</b> $\pm$ 0.2  |
| kitchen-partial-v0           | 13.1                | 18.9       | 49.8       | 46.3        | 35.5         | 33.8                                  | 57.9        | 57.0        | 12.3        | 73.3        | 66.8       | <b>76.1</b> $\pm$ 10.8 |
| Average                      | 6.6                 | 13.5       | 46.8       | 54.4        | 18.8         | 51.5                                  | 54.4        | 61.0        | 26.6        | 58.6        | 58.7       | <b>71.0</b>            |
| <b>Maze2D Tasks</b>          | <b>BEAR</b>         | <b>BCQ</b> | <b>CQL</b> | <b>IQL</b>  | <b>COMBO</b> | <b>BC</b>                             | <b>MPPI</b> | <b>DT</b>   | <b>QDT</b>  | <b>GDT</b>  | <b>DC</b>  | <b>VDT</b>             |
| maze2d-umaze-v1              | 65.7                | 49.1       | 86.7       | 42.1        | 76.4         | 85.7                                  | 33.2        | 31.0        | 57.3        | 50.4        | 20.1       | <b>88.0</b> $\pm$ 4.6  |
| maze2d-medium-v1             | 25.0                | 17.1       | 41.8       | 34.9        | 38.5         | 38.3                                  | 10.2        | 8.2         | 13.3        | 7.8         | 38.2       | <b>60.3</b> $\pm$ 0.5  |
| Average                      | 45.35               | 33.1       | 64.3       | 38.5        | 72.5         | 63.6                                  | 21.7        | 19.6        | 35.3        | 29.1        | 57.6       | <b>74.2</b>            |
| <b>AntMaze Tasks</b>         | <b>BEAR</b>         | <b>BCQ</b> | <b>CQL</b> | <b>IQL</b>  | <b>O-RL</b>  | <b>BC</b>                             | <b>DT</b>   | <b>RvS</b>  | <b>StAR</b> | <b>GDT</b>  | <b>DC</b>  | <b>VDT</b>             |
| antmaze-umaze-v0             | 73.0                | 78.9       | 74.0       | 87.1        | 64.3         | 54.6                                  | 59.2        | 65.4        | 51.3        | 76.0        | 85.0       | <b>100.0</b> $\pm$ 5.5 |
| antmaze-umaze-diverse-v0     | 61.0                | 55.0       | 84.0       | 64.4        | 60.7         | 45.6                                  | 66.2        | 60.9        | 45.6        | 69.0        | 78.5       | <b>100.0</b> $\pm$ 4.7 |
| antmaze-medium-diverse-v0    | 8.0                 | 0.0        | 53.7       | <b>70.0</b> | 0.0          | 0.0                                   | 7.5         | 67.3        | 0.0         | 0.0         | 0.0        | 30.0 $\pm$ 2.8         |
| Average                      | 47.3                | 44.6       | 70.6       | 73.8        | 41.7         | 33.4                                  | 44.3        | 75.0        | 32.3        | 48.3        | 54.5       | <b>76.7</b>            |

**Offline Training Performance.** VDT consistently achieves or approaches state-of-the-art performance across all datasets in the pure offline setting, demonstrating the effectiveness of our architecture. The Gym and Adroit environments are characterized by a limited scope of human demonstrations, which leads to extrapolation errors that particularly challenge offline RL. This is precisely why VDT’s excellent performance across all tasks can be attributed to its high expressiveness and more effective value guidance. The results of Kitchen tasks requiring generalization to unseen states and long-term

Table 2: Offline-to-online performance of each method, with average rewards reported before (left of arrow) and after (right of arrow) online tuning.

| Dataset                      | TD3+BC        | AWAC         | CQL           | IQL           | PDT                | ODT          | VDT                  |
|------------------------------|---------------|--------------|---------------|---------------|--------------------|--------------|----------------------|
| halfcheetah-medium-replay-v2 | 44.6 → 48.1   | 24.3 → 39.0  | 45.5 → 44.3   | 44.1 → 44.0   | 31.4 → 42.8        | 39.9 → 40.4  | 39.4 → <b>49.2</b>   |
| hopper-medium-replay-v2      | 60.9 → 90.7   | 77.3 → 79.6  | 95.0 → 95.3   | 92.1 → 93.5   | 84.5 → 94.8        | 86.6 → 88.9  | 96.0 → <b>119.2</b>  |
| walker2d-medium-replay-v2    | 81.8 → 82.0   | 63.8 → 44.0  | 77.2 → 78.0   | 73.7 → 60.9   | 54.5 → 79.0        | 68.9 → 76.9  | 82.3 → <b>95.5</b>   |
| halfcheetah-medium-v2        | 48.3 → 50.9   | 37.4 → 41.1  | 44.0 → 29.1   | 47.4 → 48.0   | 39.4 → <b>69.5</b> | 42.7 → 42.2  | 43.9 → 53.5          |
| hopper-medium-v2             | 59.3 → 64.6   | 72.0 → 91.0  | 58.5 → 95.7   | 63.8 → 44.3   | 74.4 → 100.2       | 66.9 → 97.5  | 98.3 → <b>108.1</b>  |
| walker2d-medium-v2           | 83.7 → 85.2   | 30.1 → 79.1  | 72.5 → 89.4   | 79.9 → 68.9   | 63.4 → 88.1        | 72.2 → 76.8  | 81.6 → <b>89.8</b>   |
| halfcheetah-medium-expert-v2 | 90.7 → 92.1   | 36.8 → 41.0  | 91.6 → 99.9   | 86.7 → 95.3   | 82.6 → 93.3        | 36.8 → 100.9 | 93.9 → <b>101.7</b>  |
| hopper-medium-expert-v2      | 98.0 → 110.2  | 80.9 → 111.9 | 105.4 → 106.3 | 91.5 → 92.9   | 77.0 → 80.0        | 74.3 → 99.1  | 111.5 → <b>117.8</b> |
| walker2d-medium-expert-v2    | 110.1 → 110.1 | 42.7 → 78.3  | 108.8 → 110.1 | 109.6 → 109.6 | 99.1 → 108.9       | 62.0 → 78.7  | 110.4 → <b>112.7</b> |
| antmaze-umaze-v0             | 78.6 → 79.1   | 56.7 → 59.0  | 70.1 → 99.4   | 86.7 → 96.0   | 48.6 → 66.8        | 53.1 → 88.5  | 100.0 → <b>110.0</b> |
| antmaze-umaze-diverse-v0     | 71.4 → 78.1   | 49.3 → 49.0  | 31.1 → 99.4   | 75.0 → 84.0   | 72.7 → 79.3        | 50.2 → 56.0  | 100.0 → <b>100.0</b> |
| antmaze-medium-diverse-v0    | 0.0 → 56.7    | 0.7 → 0.3    | 23.0 → 32.3   | 68.3 → 72.0   | 8.0 → 63.4         | 0.8 → 55.6   | 20.0 → <b>75.0</b>   |
| Average                      | 79.0          | 59.4         | 81.6          | 75.78         | 80.51              | 75.13        | <b>94.38</b>         |

Table 3: Ablation study on model components during offline training. We have abbreviated some task names for simplicity, which does not affect understanding. All experiments are repeated three times, and the average value is taken.

| Advantage Weighting | Regularization | Sampling | hopper-m    | walker-m-e   | pen-cloned   | maze2d-m    | antmaze-u    |
|---------------------|----------------|----------|-------------|--------------|--------------|-------------|--------------|
| ✓                   |                |          | 90.3        | 99.9         | 86.1         | 12.1        | 75.1         |
|                     | ✓              |          | 88.9        | 78.1         | 99.3         | 30.5        | 60.9         |
|                     |                | ✓        | 78.6        | 80.3         | 82.0         | 19.3        | 0.0          |
| ✓                   | ✓              |          | 95.6        | 103.6        | 131.8        | 40.5        | 95.9         |
| ✓                   | ✓              | ✓        | <b>98.3</b> | <b>110.4</b> | <b>145.6</b> | <b>60.3</b> | <b>100.0</b> |

value optimization demonstrate that VDT can learn useful data features from offline trajectories, enhancing generalization and stability. For the Maze2d environment, which serves as a benchmark to evaluate the capacity of algorithms to stitch segments of disparate trajectories effectively, the performance of VDT significantly outperforms other methods, demonstrating the advantage of the value functions in stitching high-quality trajectories. The AntMaze environment is characterized by sparse rewards and many suboptimal trajectories, which present an even more significant challenge. The performance results of VDT demonstrate the effectiveness and generalizability of the architecture we designed, particularly in antmaze-umaze-diverse tasks.

**Online Tuning Performance.** We conduct online tuning of VDT and observe from the results that VDT achieves optimal or competitive performance across nearly all tasks (as shown in Table 2). These results demonstrate that value-guided methods retain their advantage even in online settings. We attribute the strong performance of value-guided methods in the online setting to their ability to rapidly extract and leverage the Markovian structure of the environment through interaction. This inductive bias allows value-based approaches to adapt efficiently with limited data. In contrast, CSM lacks explicit mechanisms for modeling state transitions and thus may struggle in settings that require fast generalization from sparse interactions.

Compared to methods like ODT, which are restricted to a single setting, VDT achieves optimal performance in offline and offline-to-online scenarios. This powerfully demonstrates the inherent potential of value-guided strategies.

## 5.2 Ablation Study

**Role of Different Components.** As shown in Table 3, we conduct an ablation study on the three key components involving the value guidance in VDT. The results show that using either advantage weighting or individual regularization can improve baseline performance. However, the effectiveness varies significantly across tasks. When both components are applied together (as shown in the fourth row), performance improves substantially, suggesting that advantage weighting and regularization complement policy learning. Specifically, advantage weighting is an important form of sampling



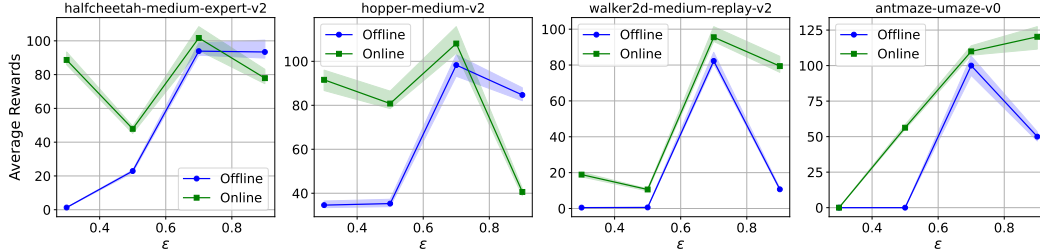


Figure 2: Ablation on the hyperparameter  $\epsilon$ .

that encourages the policy to favor high-return behaviors. At the same time, the regularization term penalizes low-value actions, effectively constraining the policy within high-value regions. Furthermore, incorporating Q-value-guided sampling enhances the stability and robustness of policy execution. When all three components are combined (as in the last row), the model achieves the best overall performance and consistency across tasks.

### Computational complexity.

Table 4 compares IQL, ODT, and VDT regarding memory usage, parameter count, and training time during offline training and online tuning. Although IQL has the lowest computational cost, it inevitably suffers from performance limitations. VDT has a slightly higher parameter count than ODT due to the introduction of the value function. However, the value-guided training process leads to faster convergence and better performance in both offline and online stages. Therefore, the slight increase in parameters is considered acceptable. VDT balances model capacity and computational efficiency well, maintaining strong representational power while significantly reducing time costs.

Table 4: Ablation on the computational complexity.

| Complexity   | Offline Training |         |         | Online Tuning |         |         |
|--------------|------------------|---------|---------|---------------|---------|---------|
|              | IQL              | ODT     | VDT     | IQL           | ODT     | VDT     |
| Memory ↓     | 960 M            | 3968 M  | 4024 M  | 960 M         | 3968 M  | 4024 M  |
| Params ↑     | 0.60 M           | 5.01 M  | 5.24 M  | 0.60 M        | 5.01 M  | 5.24 M  |
| Clock Time ↓ | ≈ 1.0 h          | ≈ 9.0 h | ≈ 5.0 h | ≈ 1.0 h       | ≈ 4.5 h | ≈ 4.0 h |

**Impact of evaluation horizon  $E$ .** We investigated the impact of the evaluation horizon during the sampling process (shown in Figure 3). Specifically, we analyzed how varying the evaluation horizon under the guidance of the value function affects model performance. It is well known that a short evaluation horizon may lead to myopic policies, while an overly long horizon can significantly slow down evaluation. Ablation studies show that a horizon length of 5 yields the best performance. Further increasing the horizon results in varying performance trends depending on the task, which is related to the dataset’s quality and the rewards’ sparsity. For simplicity, we set the evaluation horizon to 5 for all tasks.

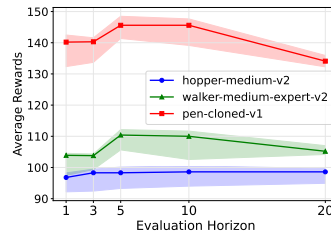


Figure 3: Ablation: Effect of Evaluation Horizon  $E$  Length on Offline Training Performance of VDT.

### Impact of context lengths $K$ .

As shown in Table 5, we observed that VDT performance improved to varying degrees with increasing context length, indicating that VDT exhibits excellent extendability. When  $K = 60$ , VDT achieved highest average performance. However, increasing context length unquestionably would significantly increase model complexity and computational cost. Considering the trade-off between performance, complexity, and ensuring fair comparison, we set  $K = 20$ .

Table 5: Offline training performance of VDT with different context lengths ( $K$ ) on Gym tasks.

| Datasets                  | VDT (8) | VDT (20)     | VDT (60)     | VDT(120) |
|---------------------------|---------|--------------|--------------|----------|
| halfcheetah-medium        | 28.6    | 43.9         | <b>44.6</b>  | 43.0     |
| hopper-medium             | 77.0    | 98.3         | <b>99.1</b>  | 65.4     |
| walker2d-medium           | 52.6    | <b>81.6</b>  | 79.9         | 80.5     |
| halfcheetah-medium-expert | 89.5    | <b>93.9</b>  | <b>93.9</b>  | 77.0     |
| hopper-medium-expert      | 109.3   | 111.5        | <b>112.7</b> | 111.2    |
| walker2d-medium-expert    | 100.6   | <b>110.4</b> | <b>110.4</b> | 103.8    |
| <b>Average</b>            | 76.3    | 89.9         | <b>90.1</b>  | 80.2     |

**Impact of hyperparameter  $\epsilon$ .** In expectile regression, the parameter  $\epsilon$  controls the value function’s preference over different TD targets. Such preference plays a crucial role in sparse reward settings or high-variance environments, as it helps prevent the policy from being misled by "lucky" samples. As shown in Figure 2, setting  $\epsilon = 0.7$  is generally effective across most tasks in both offline and online scenarios. When  $\epsilon$  approaches larger values, performance improvements are observed only on the AntMaze tasks, which we attribute to their reliance on trajectory stitching.

**Comparison with stitching baselines.** We conducted a further comparison between VDT and EDT [52], which specializes in trajectory stitching. The core idea behind EDT’s ability to stitch trajectories lies in adaptive history truncation. During inference, EDT dynamically selects the optimal history length to maximize the maximum achievable return from the current state. EDT does not use a Q-function to guide action selection. Instead, it forgets unsuccessful histories, which allows the model to escape from low-return trajectories and connect to more optimal trajectory branches. In addition, we have included a comparison with QDT [53], which combines the dynamic programming capabilities of Q-learning with the sequence modeling strengths of DT, enabling re-labeling of return targets and thus improving DT’s ability to stitch suboptimal trajectories. VDT differs in that it explicitly introduces a Q-function to provide value-guided weighting for action selection. At the same time, it employs multi-step Bellman equations and double Q-networks to stabilize value function training, thereby extending VDT to be applicable in both offline and online settings, and enabling parallel decision-making during sampling to leverage the evaluation capability of the Q-function fully. As shown in Table 6, VDT demonstrates a clear advantage over EDT and QDT across a wide range of tasks.

**Performance comparison in Atari environments.** We evaluate the proposed VDT on the image-based Atari dataset, with results averaged over three random seeds (Table 7). VDT achieves the highest average score across all considered games, substantially outperforming the prior methods CQL, DT, and DC. Specifically, VDT sets new benchmarks in the majority of tasks, evidencing its enhanced ability to handle high-dimensional visual observations. These results demonstrate that VDT possesses superior generalization capability and robustness, validating its effectiveness not only on text-based environments but also in challenging visual domains. The consistent improvements highlight the benefit of our model design in leveraging sequential and high-level representations, thereby providing a unified solution for diverse decision-making scenarios.

Table 6: Performance comparison of EDT, QDT, and VDT on Gym tasks.

| Datasets                  | EDT  | QCS  | VDT  |
|---------------------------|------|------|------|
| halfcheetah-medium        | 42.5 | 42.3 | 43.9 |
| hopper-medium             | 63.5 | 66.5 | 98.3 |
| walker2d-medium           | 72.8 | 67.1 | 81.6 |
| halfcheetah-medium-replay | 37.8 | 35.6 | 39.4 |
| hopper-medium-replay      | 89.0 | 52.1 | 96.0 |
| walker2d-medium-replay    | 74.8 | 58.2 | 82.3 |
| <b>Average</b>            | 63.4 | 53.6 | 73.6 |

Table 7: Performance Comparison in Atari Environments.

| Game           | CQL          | DT         | DC    | VDT          |
|----------------|--------------|------------|-------|--------------|
| Breakout       | 211.1        | 242.4      | 352.7 | <b>420.8</b> |
| Qbert          | <b>104.2</b> | 28.8       | 67.0  | 69.4         |
| Pong           | 111.9        | 105.6      | 106.5 | <b>113.9</b> |
| Seaquest       | 1.7          | <b>2.7</b> | 2.6   | 3.9          |
| Frostbite      | 9.4          | 25.6       | 27.8  | <b>28.9</b>  |
| <b>Average</b> | 87.7         | 81.0       | 111.3 | <b>127.4</b> |

## 6 Conclusion

In this work, we propose the Value-Guided Decision Transformer (VDT), which organically integrates policy improvement with behavior cloning, enabling efficient trajectory stitching and decision-making through components such as advantage-weighted learning and value regularization. Experiments on diverse RL benchmarks demonstrate that VDT achieves competitive performance in offline and online settings, particularly excelling in stochastic scenarios and suboptimal data regimes. This work establishes a unified CSM architecture for generalizable RL, paving the way for scalable and robust transformer-based policies in real-world applications.

**Limitation.** VDT relies on parallel trajectory evaluation during sampling, which introduces some additional computational cost, though this is generally manageable with GPU batching.

## Acknowledgments and Disclosure of Funding

This work is supported by the National Key Research and Development Program of China (2023YFC2705700), the National Natural Science Foundation of China (Grant No. 62225113, U23A20318, 62576364 and 62276195), the Foundation for Innovative Research Groups of Hubei Province (Grant No. 2024AFA017), the Science and Technology Major Project of Hubei Province (Grant No. 2024BAB046), the Shenzhen Basic Research Project (Natural Science Foundation) Basic Research Key Project (NO. JCYJ20241202124430041), the CCF-Tencent Rhino-Bird Open Research Fund (NO. CCF-Tencent RAGR20250114) and Tencent JR2025TEG002. Dr. Tao’s research is partially supported by NTU RSR and Start Up Grants. The numerical calculations in this paper have been done on the supercomputing system in the Supercomputing Center of Wuhan University.

## References

- [1] Sergey Levine, Aviral Kumar, George Tucker, and Justin Fu. Offline reinforcement learning: Tutorial, review, and perspectives on open problems. *arXiv preprint arXiv:2005.01643*, 2020.
- [2] A Vaswani. Attention is all you need. *Advances in Neural Information Processing Systems*, 2017.
- [3] Tom B Brown. Language models are few-shot learners. *arXiv preprint arXiv:2005.14165*, 2020.
- [4] Josh Achiam, Steven Adler, Sandhini Agarwal, Lama Ahmad, Ilge Akkaya, Florencia Leoni Aleman, Diogo Almeida, Janko Altmenschmidt, Sam Altman, Shyamal Anadkat, et al. Gpt-4 technical report. *arXiv preprint arXiv:2303.08774*, 2023.
- [5] Ze Liu, Yutong Lin, Yue Cao, Han Hu, Yixuan Wei, Zheng Zhang, Stephen Lin, and Baining Guo. Swin transformer: Hierarchical vision transformer using shifted windows. In *Proceedings of the IEEE/CVF international conference on computer vision*, pages 10012–10022, 2021.
- [6] Chenyang Si, Weihao Yu, Pan Zhou, Yichen Zhou, Xinchao Wang, and Shuicheng Yan. Inception transformer. *Advances in Neural Information Processing Systems*, 35:23495–23509, 2022.
- [7] Lili Chen, Kevin Lu, Aravind Rajeswaran, Kimin Lee, Aditya Grover, Misha Laskin, Pieter Abbeel, Aravind Srinivas, and Igor Mordatch. Decision transformer: Reinforcement learning via sequence modeling. *Advances in neural information processing systems*, 34:15084–15097, 2021.
- [8] Kuang-Huei Lee, Ofir Nachum, Mengjiao Sherry Yang, Lisa Lee, Daniel Freeman, Sergio Guadarrama, Ian Fischer, Winnie Xu, Eric Jang, Henryk Michalewski, et al. Multi-game decision transformers. *Advances in Neural Information Processing Systems*, 35:27921–27936, 2022.
- [9] Zhihui Xie, Zichuan Lin, Deheng Ye, Qiang Fu, Yang Wei, and Shuai Li. Future-conditioned unsupervised pretraining for decision transformer. In *International Conference on Machine Learning*, pages 38187–38203. PMLR, 2023.
- [10] Hongling Zheng, Li Shen, Yong Luo, Deheng Ye, Bo Du, Jialie Shen, and Dacheng Tao. Decision mixer: Integrating long-term and local dependencies via dynamic token selection for decision-making. In *Forty-second International Conference on Machine Learning*, 2025.
- [11] Longyang Huang, Botao Dong, and Weidong Zhang. Efficient offline reinforcement learning with relaxed conservatism. *IEEE Transactions on Pattern Analysis and Machine Intelligence*, 46(8):5260–5272, 2024.
- [12] Yuanfu Wang, Chao Yang, Ying Wen, Yu Liu, and Yu Qiao. Critic-guided decision transformer for offline reinforcement learning. In *Proceedings of the AAAI Conference on Artificial Intelligence*, pages 15706–15714, 2024.
- [13] Chen-Xiao Gao, Chenyang Wu, Mingjun Cao, Rui Kong, Zongzhang Zhang, and Yang Yu. Act: empowering decision transformer with dynamic programming via advantage conditioning. In *Proceedings of the AAAI Conference on Artificial Intelligence*, pages 12127–12135, 2024.

- [14] Philip J Ball, Laura Smith, Ilya Kostrikov, and Sergey Levine. Efficient online reinforcement learning with offline data. In *International Conference on Machine Learning*, pages 1577–1594. PMLR, 2023.
- [15] Mitsuhiro Nakamoto, Simon Zhai, Anikait Singh, Max Sobol Mark, Yi Ma, Chelsea Finn, Aviral Kumar, and Sergey Levine. Cal-ql: Calibrated offline rl pre-training for efficient online fine-tuning. *Advances in Neural Information Processing Systems*, 36:62244–62269, 2023.
- [16] Qinqing Zheng, Amy Zhang, and Aditya Grover. Online decision transformer. In *international conference on machine learning*, pages 27042–27059. PMLR, 2022.
- [17] Rishabh Agarwal, Dale Schuurmans, and Mohammad Norouzi. An optimistic perspective on offline reinforcement learning. In *International conference on machine learning*, pages 104–114. PMLR, 2020.
- [18] Shengchao Hu, Li Shen, Ya Zhang, Yixin Chen, and Dacheng Tao. On transforming reinforcement learning with transformers: The development trajectory. *IEEE Transactions on Pattern Analysis and Machine Intelligence*, 2024.
- [19] David Brandfonbrener, Alberto Bietti, Jacob Buckman, Romain Laroche, and Joan Bruna. When does return-conditioned supervised learning work for offline reinforcement learning? *Advances in Neural Information Processing Systems*, 35:1542–1553, 2022.
- [20] Hongling Zheng, Li Shen, Yong Luo, Tongliang Liu, Jialie Shen, and Dacheng Tao. Decomposed prompt decision transformer for efficient unseen task generalization. *Advances in Neural Information Processing Systems*, 37:122984–123006, 2024.
- [21] Yueh-Hua Wu, Xiaolong Wang, and Masashi Hamaya. Elastic decision transformer. *Advances in Neural Information Processing Systems*, 36, 2024.
- [22] Yevgen Chebotar, Quan Vuong, Karol Hausman, Fei Xia, Yao Lu, Alex Irpan, Aviral Kumar, Tianhe Yu, Alexander Herzog, Karl Pertsch, et al. Q-transformer: Scalable offline reinforcement learning via autoregressive q-functions. In *Conference on Robot Learning*, pages 3909–3928. PMLR, 2023.
- [23] Aviral Kumar, Aurick Zhou, George Tucker, and Sergey Levine. Conservative q-learning for offline reinforcement learning. *Advances in neural information processing systems*, 33:1179–1191, 2020.
- [24] Ilya Kostrikov, Ashvin Nair, and Sergey Levine. Offline reinforcement learning with implicit q-learning. *arXiv preprint arXiv:2110.06169*, 2021.
- [25] Siyuan Guo, Lixin Zou, Hechang Chen, Bohao Qu, Haotian Chi, S Yu Philip, and Yi Chang. Sample efficient offline-to-online reinforcement learning. *IEEE Transactions on Knowledge and Data Engineering*, 36(3):1299–1310, 2023.
- [26] Shenzhi Wang, Qisen Yang, Jiawei Gao, Matthieu Lin, Hao Chen, Liwei Wu, Ning Jia, Shiji Song, and Gao Huang. Train once, get a family: State-adaptive balances for offline-to-online reinforcement learning. *Advances in Neural Information Processing Systems*, 36:47081–47104, 2023.
- [27] Kai Zhao, Yi Ma, Jinyi Liu, Jianye Hao, Yan Zheng, and Zhaopeng Meng. Improving offline-to-online reinforcement learning with q-ensembles. In *ICML Workshop on New Frontiers in Learning, Control, and Dynamical Systems*, 2023.
- [28] Siyuan Guo, Yanchao Sun, Jifeng Hu, Sili Huang, Hechang Chen, Haiyin Piao, Lichao Sun, and Yi Chang. A simple unified uncertainty-guided framework for offline-to-online reinforcement learning. *arXiv preprint arXiv:2306.07541*, 2023.
- [29] Zhongjian Qiao, Jiafei Lyu, Kechen Jiao, Qi Liu, and Xiu Li. Sumo: Search-based uncertainty estimation for model-based offline reinforcement learning. In *Proceedings of the AAAI Conference on Artificial Intelligence*, pages 20033–20041, 2025.

- [30] Jiafei Lyu, Xiaoteng Ma, Xiu Li, and Zongqing Lu. Mildly conservative q-learning for offline reinforcement learning. *Advances in Neural Information Processing Systems*, 35:1711–1724, 2022.
- [31] Tianhe Yu, Aviral Kumar, Rafael Rafailov, Aravind Rajeswaran, Sergey Levine, and Chelsea Finn. Combo: Conservative offline model-based policy optimization. *Advances in neural information processing systems*, 34:28954–28967, 2021.
- [32] Danijar Hafner, Jurgis Pasukonis, Jimmy Ba, and Timothy Lillicrap. Mastering diverse control tasks through world models. *Nature*, pages 1–7, 2025.
- [33] Kai Yan, Alex Schwing, and Yu-Xiong Wang. Reinforcement learning gradients as vitamin for online finetuning decision transformers. *Advances in Neural Information Processing Systems*, 37:38590–38628, 2024.
- [34] Brett Daley, Martha White, and Marlos C. Machado. Averaging n-step returns reduces variance in reinforcement learning. In *Proceedings of the 41st International Conference on Machine Learning*, ICML’24. JMLR.org, 2024.
- [35] Eric Mitchell, Rafael Rafailov, Xue Bin Peng, Sergey Levine, and Chelsea Finn. Offline meta-reinforcement learning with advantage weighting. In *International Conference on Machine Learning*, pages 7780–7791. PMLR, 2021.
- [36] Kurtland Chua, Roberto Calandra, Rowan McAllister, and Sergey Levine. Deep reinforcement learning in a handful of trials using probabilistic dynamics models. *Advances in neural information processing systems*, 31, 2018.
- [37] Huayu Chen, Cheng Lu, Chengyang Ying, Hang Su, and Jun Zhu. Offline reinforcement learning via high-fidelity generative behavior modeling. In *The Eleventh International Conference on Learning Representations*, 2023.
- [38] Justin Fu, Aviral Kumar, Ofir Nachum, George Tucker, and Sergey Levine. D4rl: Datasets for deep data-driven reinforcement learning. *arXiv preprint arXiv:2004.07219*, 2020.
- [39] Aviral Kumar, Justin Fu, Matthew Soh, George Tucker, and Sergey Levine. Stabilizing off-policy q-learning via bootstrapping error reduction. *Advances in neural information processing systems*, 32, 2019.
- [40] Scott Fujimoto, David Meger, and Doina Precup. Off-policy deep reinforcement learning without exploration. In *International conference on machine learning*, pages 2052–2062. PMLR, 2019.
- [41] Rahul Kidambi, Aravind Rajeswaran, Praneeth Netrapalli, and Thorsten Joachims. Morel: Model-based offline reinforcement learning. *Advances in neural information processing systems*, 33:21810–21823, 2020.
- [42] David Brandfonbrener, Will Whitney, Rajesh Ranganath, and Joan Bruna. Offline rl without off-policy evaluation. *Advances in neural information processing systems*, 34:4933–4946, 2021.
- [43] Anurag Ajay, Yilun Du, Abhi Gupta, Joshua Tenenbaum, Tommi Jaakkola, and Pulkit Agrawal. Is conditional generative modeling all you need for decision-making? *arXiv preprint arXiv:2211.15657*, 2022.
- [44] Gaon An, Seungyong Moon, Jang-Hyun Kim, and Hyun Oh Song. Uncertainty-based offline reinforcement learning with diversified q-ensemble. *Advances in neural information processing systems*, 34:7436–7447, 2021.
- [45] Zhendong Wang, Jonathan J Hunt, and Mingyuan Zhou. Diffusion policies as an expressive policy class for offline reinforcement learning. *arXiv preprint arXiv:2208.06193*, 2022.
- [46] Jintasi Pravitra, Kasey A Ackerman, Chengyu Cao, Naira Hovakimyan, and Evangelos A Theodorou. L1-adaptive mppi architecture for robust and agile control of multirotors. In *2020 IEEE/RSJ International Conference on Intelligent Robots and Systems (IROS)*, pages 7661–7666. IEEE, 2020.

- [47] Jinghuan Shang, Kumara Kahatapitiya, Xiang Li, and Michael S Ryoo. Starformer: Transformer with state-action-reward representations for visual reinforcement learning. In *European conference on computer vision*, pages 462–479. Springer, 2022.
- [48] Shengchao Hu, Li Shen, Ya Zhang, and Dacheng Tao. Graph decision transformer. *arXiv preprint arXiv:2303.03747*, 2023.
- [49] Ashvin Nair, Abhishek Gupta, Murtaza Dalal, and Sergey Levine. Awac: Accelerating online reinforcement learning with offline datasets. *arXiv preprint arXiv:2006.09359*, 2020.
- [50] Tuomas Haarnoja, Aurick Zhou, Pieter Abbeel, and Sergey Levine. Soft actor-critic: Off-policy maximum entropy deep reinforcement learning with a stochastic actor. In *International conference on machine learning*, pages 1861–1870. Pmlr, 2018.
- [51] Scott Fujimoto and Shixiang Shane Gu. A minimalist approach to offline reinforcement learning. *Advances in neural information processing systems*, 34:20132–20145, 2021.
- [52] Yueh-Hua Wu, Xiaolong Wang, and Masashi Hamaya. Elastic decision transformer. *Advances in neural information processing systems*, 36:18532–18550, 2023.
- [53] Taku Yamagata, Ahmed Khalil, and Raul Santos-Rodriguez. Q-learning decision transformer: Leveraging dynamic programming for conditional sequence modelling in offline rl. In *International Conference on Machine Learning*, pages 38989–39007. PMLR, 2023.

## NeurIPS Paper Checklist

### 1. Claims

Question: Do the main claims made in the abstract and introduction accurately reflect the paper's contributions and scope?

Answer: [Yes]

Justification: We introduce the scope of this paper in the abstract and the Introduction section, and summarize the contribution in the Introduction section.

Guidelines:

- The answer NA means that the abstract and introduction do not include the claims made in the paper.
- The abstract and/or introduction should clearly state the claims made, including the contributions made in the paper and important assumptions and limitations. A No or NA answer to this question will not be perceived well by the reviewers.
- The claims made should match theoretical and experimental results, and reflect how much the results can be expected to generalize to other settings.
- It is fine to include aspirational goals as motivation as long as it is clear that these goals are not attained by the paper.

### 2. Limitations

Question: Does the paper discuss the limitations of the work performed by the authors?

Answer: [Yes]

Justification: We state the limitation in Section 6.

Guidelines:

- The answer NA means that the paper has no limitation while the answer No means that the paper has limitations, but those are not discussed in the paper.
- The authors are encouraged to create a separate "Limitations" section in their paper.
- The paper should point out any strong assumptions and how robust the results are to violations of these assumptions (e.g., independence assumptions, noiseless settings, model well-specification, asymptotic approximations only holding locally). The authors should reflect on how these assumptions might be violated in practice and what the implications would be.
- The authors should reflect on the scope of the claims made, e.g., if the approach was only tested on a few datasets or with a few runs. In general, empirical results often depend on implicit assumptions, which should be articulated.
- The authors should reflect on the factors that influence the performance of the approach. For example, a facial recognition algorithm may perform poorly when image resolution is low or images are taken in low lighting. Or a speech-to-text system might not be used reliably to provide closed captions for online lectures because it fails to handle technical jargon.
- The authors should discuss the computational efficiency of the proposed algorithms and how they scale with dataset size.
- If applicable, the authors should discuss possible limitations of their approach to address problems of privacy and fairness.
- While the authors might fear that complete honesty about limitations might be used by reviewers as grounds for rejection, a worse outcome might be that reviewers discover limitations that aren't acknowledged in the paper. The authors should use their best judgment and recognize that individual actions in favor of transparency play an important role in developing norms that preserve the integrity of the community. Reviewers will be specifically instructed to not penalize honesty concerning limitations.

### 3. Theory assumptions and proofs

Question: For each theoretical result, does the paper provide the full set of assumptions and a complete (and correct) proof?

Answer: [Yes]

Justification: We include the full set of assumptions and complete proofs in the appendix.

Guidelines:

- The answer NA means that the paper does not include theoretical results.
- All the theorems, formulas, and proofs in the paper should be numbered and cross-referenced.
- All assumptions should be clearly stated or referenced in the statement of any theorems.
- The proofs can either appear in the main paper or the supplemental material, but if they appear in the supplemental material, the authors are encouraged to provide a short proof sketch to provide intuition.
- Inversely, any informal proof provided in the core of the paper should be complemented by formal proofs provided in appendix or supplemental material.
- Theorems and Lemmas that the proof relies upon should be properly referenced.

#### 4. Experimental result reproducibility

Question: Does the paper fully disclose all the information needed to reproduce the main experimental results of the paper to the extent that it affects the main claims and/or conclusions of the paper (regardless of whether the code and data are provided or not)?

Answer: [Yes]

Justification: We provide a detailed experimental description in the main text and the appendix. All the datasets, code, and model checkpoints are publicly available.

Guidelines:

- The answer NA means that the paper does not include experiments.
- If the paper includes experiments, a No answer to this question will not be perceived well by the reviewers: Making the paper reproducible is important, regardless of whether the code and data are provided or not.
- If the contribution is a dataset and/or model, the authors should describe the steps taken to make their results reproducible or verifiable.
- Depending on the contribution, reproducibility can be accomplished in various ways. For example, if the contribution is a novel architecture, describing the architecture fully might suffice, or if the contribution is a specific model and empirical evaluation, it may be necessary to either make it possible for others to replicate the model with the same dataset, or provide access to the model. In general, releasing code and data is often one good way to accomplish this, but reproducibility can also be provided via detailed instructions for how to replicate the results, access to a hosted model (e.g., in the case of a large language model), releasing of a model checkpoint, or other means that are appropriate to the research performed.
- While NeurIPS does not require releasing code, the conference does require all submissions to provide some reasonable avenue for reproducibility, which may depend on the nature of the contribution. For example
  - (a) If the contribution is primarily a new algorithm, the paper should make it clear how to reproduce that algorithm.
  - (b) If the contribution is primarily a new model architecture, the paper should describe the architecture clearly and fully.
  - (c) If the contribution is a new model (e.g., a large language model), then there should either be a way to access this model for reproducing the results or a way to reproduce the model (e.g., with an open-source dataset or instructions for how to construct the dataset).
  - (d) We recognize that reproducibility may be tricky in some cases, in which case authors are welcome to describe the particular way they provide for reproducibility. In the case of closed-source models, it may be that access to the model is limited in some way (e.g., to registered users), but it should be possible for other researchers to have some path to reproducing or verifying the results.

#### 5. Open access to data and code

Question: Does the paper provide open access to the data and code, with sufficient instructions to faithfully reproduce the main experimental results, as described in supplemental material?



Answer: [Yes]

Justification: All the datasets, code, and model checkpoints are publicly available.

Guidelines:

- The answer NA means that paper does not include experiments requiring code.
- Please see the NeurIPS code and data submission guidelines (<https://nips.cc/public/guides/CodeSubmissionPolicy>) for more details.
- While we encourage the release of code and data, we understand that this might not be possible, so “No” is an acceptable answer. Papers cannot be rejected simply for not including code, unless this is central to the contribution (e.g., for a new open-source benchmark).
- The instructions should contain the exact command and environment needed to run to reproduce the results. See the NeurIPS code and data submission guidelines (<https://nips.cc/public/guides/CodeSubmissionPolicy>) for more details.
- The authors should provide instructions on data access and preparation, including how to access the raw data, preprocessed data, intermediate data, and generated data, etc.
- The authors should provide scripts to reproduce all experimental results for the new proposed method and baselines. If only a subset of experiments are reproducible, they should state which ones are omitted from the script and why.
- At submission time, to preserve anonymity, the authors should release anonymized versions (if applicable).
- Providing as much information as possible in supplemental material (appended to the paper) is recommended, but including URLs to data and code is permitted.

## 6. Experimental setting/details

Question: Does the paper specify all the training and test details (e.g., data splits, hyper-parameters, how they were chosen, type of optimizer, etc.) necessary to understand the results?

Answer: [Yes]

Justification: Yes, both in the main paper and in the appendix.

Guidelines:

- The answer NA means that the paper does not include experiments.
- The experimental setting should be presented in the core of the paper to a level of detail that is necessary to appreciate the results and make sense of them.
- The full details can be provided either with the code, in appendix, or as supplemental material.

## 7. Experiment statistical significance

Question: Does the paper report error bars suitably and correctly defined or other appropriate information about the statistical significance of the experiments?

Answer: [Yes]

Justification: We provide standard deviations in numerical form in Table 1. Additionally, the visualization results in the ablation study section include standard deviations represented as shaded areas.

Guidelines:

- The answer NA means that the paper does not include experiments.
- The authors should answer "Yes" if the results are accompanied by error bars, confidence intervals, or statistical significance tests, at least for the experiments that support the main claims of the paper.
- The factors of variability that the error bars are capturing should be clearly stated (for example, train/test split, initialization, random drawing of some parameter, or overall run with given experimental conditions).
- The method for calculating the error bars should be explained (closed form formula, call to a library function, bootstrap, etc.)
- The assumptions made should be given (e.g., Normally distributed errors).

- It should be clear whether the error bar is the standard deviation or the standard error of the mean.
- It is OK to report 1-sigma error bars, but one should state it. The authors should preferably report a 2-sigma error bar than state that they have a 96% CI, if the hypothesis of Normality of errors is not verified.
- For asymmetric distributions, the authors should be careful not to show in tables or figures symmetric error bars that would yield results that are out of range (e.g. negative error rates).
- If error bars are reported in tables or plots, The authors should explain in the text how they were calculated and reference the corresponding figures or tables in the text.

#### 8. Experiments compute resources

Question: For each experiment, does the paper provide sufficient information on the computer resources (type of compute workers, memory, time of execution) needed to reproduce the experiments?

Answer: [Yes]

Justification: We provide the information in ablation study section.

Guidelines:

- The answer NA means that the paper does not include experiments.
- The paper should indicate the type of compute workers CPU or GPU, internal cluster, or cloud provider, including relevant memory and storage.
- The paper should provide the amount of compute required for each of the individual experimental runs as well as estimate the total compute.
- The paper should disclose whether the full research project required more compute than the experiments reported in the paper (e.g., preliminary or failed experiments that didn't make it into the paper).

#### 9. Code of ethics

Question: Does the research conducted in the paper conform, in every respect, with the NeurIPS Code of Ethics [https://neurips.cc/public/EthicsGuidelines?](https://neurips.cc/public/EthicsGuidelines)

Answer: [Yes]

Justification: The research conducted in the paper fully conforms to the NeurIPS Code of Ethics.

Guidelines:

- The answer NA means that the authors have not reviewed the NeurIPS Code of Ethics.
- If the authors answer No, they should explain the special circumstances that require a deviation from the Code of Ethics.
- The authors should make sure to preserve anonymity (e.g., if there is a special consideration due to laws or regulations in their jurisdiction).

#### 10. Broader impacts

Question: Does the paper discuss both potential positive societal impacts and negative societal impacts of the work performed?

Answer: [NA]

Justification: There is no societal impact of the work performed.

Guidelines:

- The answer NA means that there is no societal impact of the work performed.
- If the authors answer NA or No, they should explain why their work has no societal impact or why the paper does not address societal impact.
- Examples of negative societal impacts include potential malicious or unintended uses (e.g., disinformation, generating fake profiles, surveillance), fairness considerations (e.g., deployment of technologies that could make decisions that unfairly impact specific groups), privacy considerations, and security considerations.

- The conference expects that many papers will be foundational research and not tied to particular applications, let alone deployments. However, if there is a direct path to any negative applications, the authors should point it out. For example, it is legitimate to point out that an improvement in the quality of generative models could be used to generate deepfakes for disinformation. On the other hand, it is not needed to point out that a generic algorithm for optimizing neural networks could enable people to train models that generate Deepfakes faster.
- The authors should consider possible harms that could arise when the technology is being used as intended and functioning correctly, harms that could arise when the technology is being used as intended but gives incorrect results, and harms following from (intentional or unintentional) misuse of the technology.
- If there are negative societal impacts, the authors could also discuss possible mitigation strategies (e.g., gated release of models, providing defenses in addition to attacks, mechanisms for monitoring misuse, mechanisms to monitor how a system learns from feedback over time, improving the efficiency and accessibility of ML).

## 11. Safeguards

Question: Does the paper describe safeguards that have been put in place for responsible release of data or models that have a high risk for misuse (e.g., pretrained language models, image generators, or scraped datasets)?

Answer: [NA]

Justification: The paper poses no such risks.

Guidelines:

- The answer NA means that the paper poses no such risks.
- Released models that have a high risk for misuse or dual-use should be released with necessary safeguards to allow for controlled use of the model, for example by requiring that users adhere to usage guidelines or restrictions to access the model or implementing safety filters.
- Datasets that have been scraped from the Internet could pose safety risks. The authors should describe how they avoided releasing unsafe images.
- We recognize that providing effective safeguards is challenging, and many papers do not require this, but we encourage authors to take this into account and make a best faith effort.

## 12. Licenses for existing assets

Question: Are the creators or original owners of assets (e.g., code, data, models), used in the paper, properly credited and are the license and terms of use explicitly mentioned and properly respected?

Answer: [Yes]

Justification: We have properly credited the creators and original owners of all assets used in the paper through citations and other appropriate means, ensuring that the licenses and terms of use are respected.

Guidelines:

- The answer NA means that the paper does not use existing assets.
- The authors should cite the original paper that produced the code package or dataset.
- The authors should state which version of the asset is used and, if possible, include a URL.
- The name of the license (e.g., CC-BY 4.0) should be included for each asset.
- For scraped data from a particular source (e.g., website), the copyright and terms of service of that source should be provided.
- If assets are released, the license, copyright information, and terms of use in the package should be provided. For popular datasets, [paperswithcode.com/datasets](https://paperswithcode.com/datasets) has curated licenses for some datasets. Their licensing guide can help determine the license of a dataset.

- For existing datasets that are re-packaged, both the original license and the license of the derived asset (if it has changed) should be provided.
- If this information is not available online, the authors are encouraged to reach out to the asset’s creators.

### 13. **New assets**

Question: Are new assets introduced in the paper well documented and is the documentation provided alongside the assets?

Answer: [NA]

Justification: The paper does not release new assets.

Guidelines:

- The answer NA means that the paper does not release new assets.
- Researchers should communicate the details of the dataset/code/model as part of their submissions via structured templates. This includes details about training, license, limitations, etc.
- The paper should discuss whether and how consent was obtained from people whose asset is used.
- At submission time, remember to anonymize your assets (if applicable). You can either create an anonymized URL or include an anonymized zip file.

### 14. **Crowdsourcing and research with human subjects**

Question: For crowdsourcing experiments and research with human subjects, does the paper include the full text of instructions given to participants and screenshots, if applicable, as well as details about compensation (if any)?

Answer: [NA]

Justification: The paper does not involve crowdsourcing nor research with human subjects.

Guidelines:

- The answer NA means that the paper does not involve crowdsourcing nor research with human subjects.
- Including this information in the supplemental material is fine, but if the main contribution of the paper involves human subjects, then as much detail as possible should be included in the main paper.
- According to the NeurIPS Code of Ethics, workers involved in data collection, curation, or other labor should be paid at least the minimum wage in the country of the data collector.

### 15. **Institutional review board (IRB) approvals or equivalent for research with human subjects**

Question: Does the paper describe potential risks incurred by study participants, whether such risks were disclosed to the subjects, and whether Institutional Review Board (IRB) approvals (or an equivalent approval/review based on the requirements of your country or institution) were obtained?

Answer: [NA]

Justification: The paper does not involve crowdsourcing nor research with human subjects.

Guidelines:

- The answer NA means that the paper does not involve crowdsourcing nor research with human subjects.
- Depending on the country in which research is conducted, IRB approval (or equivalent) may be required for any human subjects research. If you obtained IRB approval, you should clearly state this in the paper.
- We recognize that the procedures for this may vary significantly between institutions and locations, and we expect authors to adhere to the NeurIPS Code of Ethics and the guidelines for their institution.
- For initial submissions, do not include any information that would break anonymity (if applicable), such as the institution conducting the review.

#### 16. Declaration of LLM usage

Question: Does the paper describe the usage of LLMs if it is an important, original, or non-standard component of the core methods in this research? Note that if the LLM is used only for writing, editing, or formatting purposes and does not impact the core methodology, scientific rigorousness, or originality of the research, declaration is not required.

Answer: [NA]

Justification: The core method development in this research does not involve LLMs as any important, original, or non-standard components.

Guidelines:

- The answer NA means that the core method development in this research does not involve LLMs as any important, original, or non-standard components.
- Please refer to our LLM policy (<https://neurips.cc/Conferences/2025/LLM>) for what should or should not be described.

## Appendix

The appendix is organized into several sections, each providing additional insights and details related to different aspects of the main work.

|  |           |
|--|-----------|
| <b>A Proof of Theroem 4.1</b>          | <b>22</b> |
| <b>B Proof of Theroem 4.2</b>          | <b>23</b> |
| <b>C Hyperparameters Configuration</b> | <b>24</b> |
| <b>D Algorithm Pseudocode</b>          | <b>24</b> |
| <b>E Environment Details</b>           | <b>25</b> |
| <b>F More Experiments</b>              | <b>27</b> |
| <b>G Broader Impact</b>                | <b>30</b> |

---

### A Proof of Theroem 4.1

Let  $\pi_{DT}^*$  be the optimal policy obtained by solving Equation 5. For any  $s \in S$ , we have:

1. **Support Constraint:**  $\pi_{DT}^*(s) \in \text{supp}(\beta(\cdot|s))$ ,
2. **Value Improvement:**  $V^{\pi_{DT}^*}(s) \geq V^\beta(s)$ ,

where  $\text{supp}(\beta(\cdot|s)) = \{a \in \mathcal{A} \mid \exists(s, a) \in \mathcal{D}\}$ , and  $\pi^*(\mathbf{a} \mid \mathbf{s}) = 0$  whenever  $\beta(\mathbf{a} \mid \mathbf{s}) = 0$ .

**Lemma A.1** (Implicit Support Constraint). *The policy gradient update satisfies:*

$$\nabla \mathcal{L}(\pi_{DT}^{(d)}) = \mathbb{E}_{\mathcal{D}} \left[ 2e^{\eta A_t} (\pi_{DT}^{(d)}(\tau_t) - a_t) - \lambda \nabla_a Q_{\hat{\theta}}(s_t, a) \Big|_{a=\pi_{DT}^{(d)}(\tau_t)} \right], \quad (7)$$

where all gradient components vanish outside  $\text{supp}(\beta(\cdot|s))$ .

**Lemma A.2** (Policy Improvement). *The advantage-weighted value function [35] satisfies:*

$$\tilde{V}^{\pi_{DT}^{(d+1)}}(s) \geq \tilde{V}^{\pi_{DT}^{(d)}}(s) + \frac{\lambda}{1-\gamma} \mathbb{E}_{\mathcal{D}} \left[ \min_i Q_{\hat{\theta}_i}(s, \pi_{DT}^{(d+1)}(s)) \right]. \quad (8)$$

*Proof.* Define the policy optimization sequence  $\{\pi_{DT}^{(d)}\}_{d=0}^\infty$  where  $d$  denotes training iterations, with  $\pi_{DT}^{(0)} = \beta$ . We prove each statement in turn.

**(1) Support Constraint:** From the gradient expression in Lemma A.1, the policy update rule is given by:

$$\nabla \mathcal{L}(\pi_{DT}^{(d)}) = \mathbb{E}_{\mathcal{D}} \left[ 2e^{\eta A_t} (\pi_{DT}^{(d)}(\tau_t) - a_t) - \lambda \nabla_a Q_{\hat{\theta}}(s_t, a) \Big|_{a=\pi_{DT}^{(d)}(\tau_t)} \right], \quad (9)$$

where all terms are evaluated only on trajectories  $(s_t, a_t)$  from the dataset  $\mathcal{D}$ . The gradient thus vanishes outside  $\text{supp}(\beta(\cdot|s))$ .

Moreover, the behavior cloning component implicitly restricts  $\pi_{DT}^{(d)}(s)$  to lie within the convex hull of actions observed in the dataset:

$$\pi_{DT}^*(s) = \lim_{d \rightarrow \infty} \text{Proj}_{\mathcal{A}_{\mathcal{D}}(s)} \left( \pi_{DT}^{(d)}(s) \right), \quad (10)$$

where  $\mathcal{A}_{\mathcal{D}}(s) := \{a \mid (s, a) \in \mathcal{D}\}$ . In addition, the Q-regularization term enforces vanishing gradients near the boundary of this set, preventing the policy from drifting outside. Hence, the optimal policy satisfies the support constraint.

**(2) Value Improvement:** Define the value gap at iteration  $d$  as:

$$\epsilon^{(d)} := V^*(s) - \tilde{V}^{\pi^{(d)}}(s), \quad (11)$$

where  $\tilde{V}^{\pi}$  denotes the advantage-weighted surrogate value used in the optimization.

From Lemma A.2, the policy update guarantees monotonic improvement:

$$\tilde{V}^{\pi^{(d+1)}}(s) \geq \tilde{V}^{\pi^{(d)}}(s) + \frac{\lambda}{1-\gamma} \mathbb{E}_{\mathcal{D}} \left[ \min_i Q_{\hat{\theta}_i}(s, \pi_{DT}^{(d+1)}(s)) \right]. \quad (12)$$

Applying the  $n$ -step Bellman operator  $\mathcal{T}^n$  yields:

$$\epsilon^{(d+1)} \leq \gamma^n \epsilon^{(d)} - \lambda \mathbb{E}_{\mathcal{D}} \left[ \min_i Q_{\hat{\theta}_i}(s, \pi_{DT}^{(d+1)}(s)) \right] \leq \gamma^n \epsilon^{(d)} - \lambda \left( V^{\pi_{DT}^{(d+1)}}(s) - V^{\beta}(s) \right), \quad (13)$$

where we used that  $\min_i Q_{\hat{\theta}_i}$  lower bounds the true  $V^{\pi_{DT}^{(d+1)}}$  and that  $V^{\beta}$  is the value under the behavior policy.

Telescoping this recurrence and assuming convergence as  $d \rightarrow \infty$ , we obtain:

$$V^{\pi_{DT}^*}(s) \geq V^{\beta}(s). \quad (14)$$

The inequality is strict unless the Q-functions are constant over  $\mathcal{A}_D(s)$ , in which case the behavior policy  $\beta$  is already optimal within the dataset support.

## B Proof of Theorem 4.2

Let  $\pi^*$  denote the globally optimal policy and  $\pi_{DT}^*$  denote the optimal policy constrained to dataset support. Define  $\mathcal{A}_D(s) := \{a \mid (s, a) \in \mathcal{D}\}$  to be the set of actions observed in the dataset at state  $s$ . For any  $s$ , we have:

$$V^{\pi^*}(\mu) - V^{\pi_{DT}^*}(\mu) \leq \frac{2\gamma}{(1-\gamma)^2} \mathbb{E}_{s \sim d^{\pi^*}} \left[ \max_{a \notin \mathcal{A}_D(s)} Q^{\pi^*}(s, a) - \max_{a \in \text{supp}(\beta(\cdot|s))} Q^{\pi^*}(s, a) \right] \quad (15)$$

*Proof. Step 1: Performance Difference Lemma*

Recall for any two policies  $\pi, \pi'$ , the performance difference lemma states:

$$V^{\pi}(\mu) - V^{\pi'}(\mu) = \frac{1}{1-\gamma} \mathbb{E}_{s \sim d^{\pi}} \left[ \mathbb{E}_{a \sim \pi(\cdot|s)} \left[ Q^{\pi'}(s, a) - V^{\pi'}(s) \right] \right] \quad (16)$$

where  $d^{\pi}(s)$  is the normalized discounted state distribution under  $\pi$ .

**Step 2: Comparing  $\pi^*$  and  $\pi_{DT}^*$**

Applying the lemma yields:

$$V^{\pi^*}(\mu) - V^{\pi_{DT}^*}(\mu) = \frac{1}{1-\gamma} \mathbb{E}_{s \sim d^{\pi^*}} \left[ \mathbb{E}_{a \sim \pi^*(\cdot|s)} \left[ Q^{\pi_{DT}^*}(s, a) - V^{\pi_{DT}^*}(s) \right] \right] \quad (17)$$

$$\leq \frac{1}{1-\gamma} \mathbb{E}_{s \sim d^{\pi^*}} \left[ \max_a Q^{\pi_{DT}^*}(s, a) - \max_{a \in \mathcal{A}_D(s)} Q^{\pi_{DT}^*}(s, a) \right] \quad (18)$$

since  $\pi^*$  may select actions  $a^* \notin \mathcal{A}_D(s)$  that  $\pi_{DT}^*$  cannot, incurring a value gap.

**Step 3: Relating  $Q^{\pi_{DT}^*}$  to  $Q^{\pi^*}$**

Since  $Q^{\pi_{DT}^*}(s, a) \leq Q^{\pi^*}(s, a)$  for all  $a$ , we may further bound:

$$V^{\pi_{DT}^*}(s) = \max_{a \in \mathcal{A}_D(s)} Q^{\pi_{DT}^*}(s, a) \leq \max_{a \in \mathcal{A}_D(s)} Q^{\pi^*}(s, a) \quad (19)$$

and

$$V^{\pi^*}(s) = \max_a Q^{\pi^*}(s, a) \quad (20)$$

At each state  $s$ , the maximal loss incurred is thus

$$\delta(s) := V^{\pi^*}(s) - \max_{a \in \mathcal{A}_D(s)} Q^{\pi^*}(s, a) = \max_a Q^{\pi^*}(s, a) - \max_{a \in \mathcal{A}_D(s)} Q^{\pi^*}(s, a) \quad (21)$$

#### Step 4: Cumulative suboptimality by recursion

Because  $\pi_{DT}^*$  can only select actions within the dataset support at each step, the loss  $\delta(s_t)$  compounds over all timesteps. By recursive expansion and geometric series, we obtain:

$$V^{\pi^*}(\mu) - V^{\pi_{DT}^*}(\mu) \leq \frac{1}{1-\gamma} \mathbb{E}_{s \sim d^{\pi^*}} [\delta(s)] + \frac{\gamma}{1-\gamma} \mathbb{E}_{s \sim d^{\pi^*}} [\delta(s)] + \dots \quad (22)$$

Summing the geometric series yields:

$$V^{\pi^*}(\mu) - V^{\pi_{DT}^*}(\mu) \leq \frac{1}{(1-\gamma)^2} \mathbb{E}_{s \sim d^{\pi^*}} [\delta(s)] \quad (23)$$

By a refinement [40], accounting for effect propagation across steps, a factor  $2\gamma$  appears:

$$V^{\pi^*}(\mu) - V^{\pi_{DT}^*}(\mu) \leq \frac{2\gamma}{(1-\gamma)^2} \mathbb{E}_{s \sim d^{\pi^*}} [\delta(s)] \quad (24)$$

Thus, we have proven

$$V^{\pi^*}(\mu) - V^{\pi_{DT}^*}(\mu) \leq \frac{2\gamma}{(1-\gamma)^2} \mathbb{E}_{s \sim d^{\pi^*}} \left[ \max_{a \notin \mathcal{A}_D(s)} Q^{\pi^*}(s, a) - \max_{a \in \text{supp}(\beta(\cdot|s))} Q^{\pi^*}(s, a) \right] \quad (25)$$

which bounds the loss in optimal value due to dataset support constraints.

## C Hyperparameters Configuration

Table 8: Hyperparameter configurations for offline training and online tuning.

| Hyperparameter                | Offline Training | Online Tuning |
|-------------------------------|------------------|---------------|
| Context Length $K$            | 20               | 20            |
| Batch Size                    | 512              | 512           |
| Training Steps                | 10000            | 25000         |
| Learning Rate                 | 3e-4             | 1e-4          |
| Weight Decay                  | 1e-4             | —             |
| Number of Layers              | 6                | 6             |
| Attention Heads               | 4                | 4             |
| Embedding Dimension           | 256              | 256           |
| Activation                    | GeLU             | GeLU          |
| Dropout                       | 0.1              | 0.1           |
| Discount $\gamma$             | 0.99             | 0.99          |
| Threshold $\epsilon$          | 0.7              | 0.7           |
| Inverse Temperature $\eta$    | 3                | 3             |
| Balance Coefficient $\lambda$ | 0.5              | 0.5           |
| pct_traj                      | 1                | 1             |
| Updates between Rollouts      | —                | 300           |
| Gradient Norm Clip            | 0.25             | 0.25          |
| Replay Buffer Size            | —                | 1000          |
| Q-network Layers              | 2                | 2             |
| Q-network Width               | 256              | 256           |

## D Algorithm Pseudocode



---

**Algorithm 1** Offline Training with VDT

---

**Input:** Offline dataset  $\mathcal{D}_{\text{offline}}$ , Context length  $K$ , Expectile  $\epsilon$ , Discount  $\gamma, \lambda, \eta$   
**Initialize:**  $\pi_{DT}, V_\psi, Q_{\theta_1}, Q_{\theta_2}, Q_{\hat{\theta}_1}, Q_{\hat{\theta}_2}$   
**for** iteration = 1 to  $T$  **do**  
  Sample batch  $\mathcal{B} \sim \mathcal{D}_{\text{offline}}$   
  {Value network update}  
  Update  $V_\psi$  using:  $\mathbb{E}_{(s,a) \sim \mathcal{B}}[L_2^\epsilon(Q_{\hat{\theta}}(s, a) - V_\psi(s))]$   
  {Q-network update}  
  Compute n-step targets:  $y = \sum_{k=0}^{n-1} \gamma^k r_k + \gamma^n V_\psi(s_{t+n})$   
  Update  $Q_{\theta_i}$  using:  $\mathbb{E}_{\mathcal{B}}[(y - Q_{\theta_i}(s_t, a_t))^2]$  for  $i = 1, 2$   
  {Advantage-weighted policy update}  
  Compute advantages:  $A_t = \min_i Q_{\hat{\theta}_i}(s_t, a_t) - V_\psi(s_t)$   
  Update  $\pi_{DT}$  using:  
     $\mathbb{E}_{\mathcal{B}}[\exp(\eta A_t) \|\pi_{DT}(\tau_t) - a_t\|^2 - \lambda \min_i Q_{\hat{\theta}_i}(s_t, \pi_{DT}(\tau_t))]$   
  {Target network update}  
   $\hat{\theta}_i \leftarrow \rho \hat{\theta}_i + (1 - \rho) \theta_i$  for  $i = 1, 2$   
**end for**

---

---

**Algorithm 2** Online Tuning with Trajectory Replay

---

**Input:** Pretrained  $\pi_{DT}, Q_{\hat{\theta}_i}$ , Online RTG  $g_{\text{online}}$ , Buffer size  $N$ , Context length  $K$   
Initialize replay buffer  $\mathcal{T}_{\text{replay}} \leftarrow \text{Top-}N(\mathcal{D}_{\text{offline}})$   
**for** round = 1 to  $R$  **do**  
  Generate trajectory  $\tau$  with  $\pi_{DT}$  using  $g_{\text{online}}$   
  Relabel RTG:  $g_t = \sum_{j=t}^{|\tau|} r_j$  for  $t \in \tau$   
  Update  $\mathcal{T}_{\text{replay}}$  (FIFO)  
  **for** gradient step = 1 to  $I$  **do**  
    Sample trajectories  $\{\tau_j\} \sim \mathcal{T}_{\text{replay}}$  with  $p(\tau) \propto |\tau|$   
    **for** each  $\tau_j$  **do**  
      Sample sub-trajectory  $(\hat{s}_{t:t+K}, \hat{a}_{t:t+K}, \hat{g}_{t:t+K})$   
      Compute  $A_t = \min_i Q_{\hat{\theta}_i}(\hat{s}_t, \hat{a}_t) - V_\psi(\hat{s}_t)$   
    **end for**  
    Update  $\pi_{DT}$  using:  
       $\frac{1}{B} \sum \left[ \exp(\eta A_t) \|\pi_{DT}(\hat{s}_t, \hat{g}_t) - \hat{a}_t\|^2 - \lambda \min_i Q_{\hat{\theta}_i}(\hat{s}_t, \pi_{DT}(\hat{s}_t, \hat{g}_t)) \right]$   
    Update  $Q_{\theta_i}$  using online transitions  
     $\hat{\theta}_i \leftarrow \rho \hat{\theta}_i + (1 - \rho) \theta_i$   
  **end for**  
**end for**

---

## E Environment Details

**Gym tasks:** The Gym-MuJoCo tasks (hopper, halfcheetah, walker2d) are popular benchmarks used in offline deep RL. They are relatively straightforward and characterized by datasets with a significant proportion of near-optimal trajectories and smooth reward functions. The "medium" dataset is generated by first training a policy online using Soft Actor-Critic, early-stopping the training, and collecting 1M samples from this partially-trained policy. The "random" datasets are generated by unrolling a randomly initialized policy on these three domains. The "medium-replay" dataset consists of recording all samples in the replay buffer observed during training until the policy reaches the "medium" level of performance. Datasets similar to these three have been used in prior work, but in order to evaluate algorithms on mixtures of policies, we further introduce a "medium-expert" dataset by mixing equal amounts of expert demonstrations and suboptimal data, generated via a partially trained policy or by unrolling a uniform-at-random policy.

**Adroit tasks:** The Adroit domain involves controlling a 24-DoF simulated Shadow Hand robot to perform tasks such as hammering a nail, opening a door, twirling a pen, or picking up and moving a ball. This domain is chosen to study the impact of narrow expert data distributions and human

---

**Algorithm 3** Sampling Process
 

---

**Input:** Initial state  $s_0$ , candidate RTGs  $\{\hat{r}_0^1, \dots, \hat{r}_0^m\}$ , Evaluation horizon  $E$ , Discount  $\gamma$ , Policy  $\pi_{DT}$ , Q-networks  $Q_{\hat{\theta}_1}, Q_{\hat{\theta}_2}$

**Initialize:** Current state  $s_t \leftarrow s_0$ , Active trajectories  $\{\tau^k\}_{k=1}^m \leftarrow \{(s_0, \hat{r}_0^k)\}_{k=1}^m$ , Target Q-networks  $Q_{\hat{\theta}_i}$

**while** not termination condition **do**

*// Parallel candidate action generation*

**for**  $k = 1$  **to**  $m$  **in parallel** **do**

Sample action  $a_t^k \sim \pi_{DT}(\tau^k)$

**end for**

*// Batched trajectory prediction*

**for**  $k = 1$  **to**  $m$  **in parallel** **do**

Initialize predicted trajectory  $\tau_{\text{pred}}^k \leftarrow (s_t, a_t^k)$

Initialize cumulative Q-value  $Q_{\text{total}}^k \leftarrow 0$

**for**  $i = 0$  **to**  $E - 1$  **do**

Predict next state:  $s_{t+i+1}^k \leftarrow \text{EnvModel}(\tau_{\text{pred}}^k)$

Sample next action:  $a_{t+i+1}^k \sim \pi_{DT}(\tau_{\text{pred}}^k)$

Compute Q-value:  $q_i^k = \min_{j=1,2} Q_{\hat{\theta}_j}(s_{t+i}^k, a_{t+i}^k)$

Accumulate:  $Q_{\text{total}}^k \leftarrow Q_{\text{total}}^k + \gamma^i q_i^k$

Append  $(a_{t+i+1}^k, s_{t+i+1}^k)$  to  $\tau_{\text{pred}}^k$

**end for**

**end for**

*// Optimal action selection*

Select optimal index:  $k^* \leftarrow \arg \max_{1 \leq k \leq m} Q_{\text{total}}^k$

Execute action:  $a_t \leftarrow a_t^{k^*}$

*// Environment interaction & trajectory update*

Observe reward  $r_t$ , next state  $s_{t+1}$  from environment

**for**  $k = 1$  **to**  $m$  **do**

Update RTG:  $\hat{r}_{t+1}^k \leftarrow \hat{r}_t^k - r_t$

Append transition:  $\tau^k \leftarrow \tau^k \oplus (a_t, r_t, s_{t+1}, \hat{r}_{t+1}^k)$

**end for**

$t \leftarrow t + 1$

**end while**

---

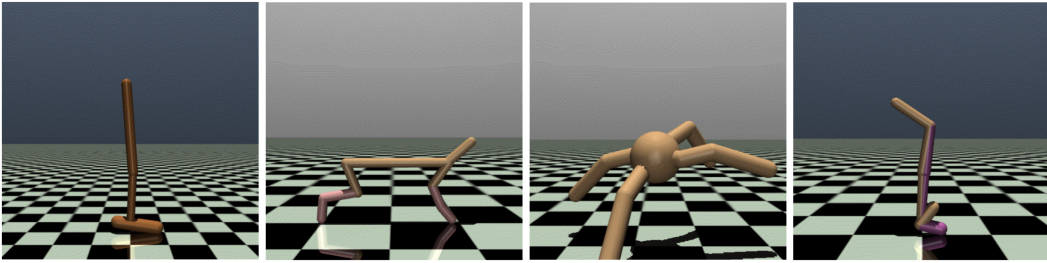


Figure 4: Illustration of Gym environments [38].

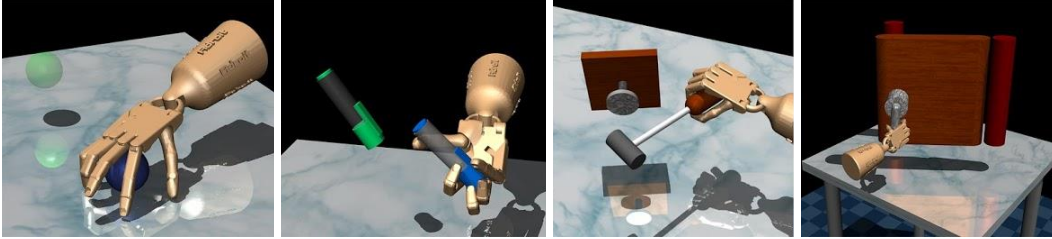


Figure 5: Illustration of Adroit environments [38].

demonstrations on sparse-reward, high-dimensional robotic manipulation tasks. Since these tasks are primarily derived from human behavior, they exhibit a limited state-action space, requiring robust policy regularization to ensure consistent agent performance. The Adroit domain has several unique properties that make it qualitatively different from the Gym tasks. First, the data is collected from human demonstrators. Second, each task is difficult to solve with online RL due to sparse rewards and exploration challenges, which make cloning and online RL alone insufficient. Lastly, the tasks are high-dimensional, presenting a representation learning challenge.

**Kitchen tasks:** The Kitchen domain involves controlling a 9-DoF Franka robot in a kitchen environment with everyday household items such as a microwave, kettle, overhead light, cabinets, and an oven. The goal is to interact with these items to achieve a desired state configuration. This domain benchmarks the impact of multitasking behaviour in a realistic, non-navigation environment, where the "stitching" challenge arises from complex paths through the state space. Consequently, algorithms must generalize to unseen states rather than rely solely on training trajectories. The environment requires the agent to complete multiple sequential sub-tasks, further emphasizing the need for robust generalization. The "complete" dataset consists of the robot performing all the desired tasks in order. This provides data that is easy for an imitation learning method to solve. The "partial" dataset consists of undirected data, where the robot performs subtasks that are not necessarily related to the goal configuration. In the "partial" dataset, a subset is guaranteed to solve the task, meaning an imitation learning agent may learn by selectively choosing the proper subsets of the data.

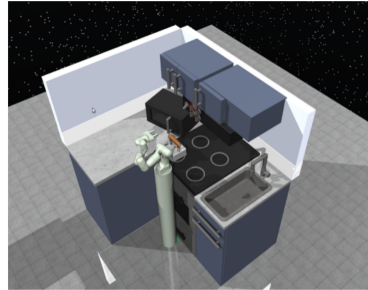


Figure 6: Illustration of Kitchen environments [38].

**Maze2D tasks:** The Maze2D domain is a navigation task in which a 2D agent must reach a fixed goal location. It tests offline RL algorithms' ability to stitch together previously collected sub-trajectories to find the shortest path to the goal. Three maze layouts are provided: the "maze", "medium", and "large" mazes. These tasks evaluate the algorithm's capability to effectively combine sub-trajectories and identify the shortest path to the set goal. The data is generated by selecting goal locations randomly and then using a planner that generates sequences of waypoints, followed by a PD controller. The trajectories in the dataset are visualized in Appendix G. Because the controllers memorize the reached waypoints, the data collection policy is non-Markovian.

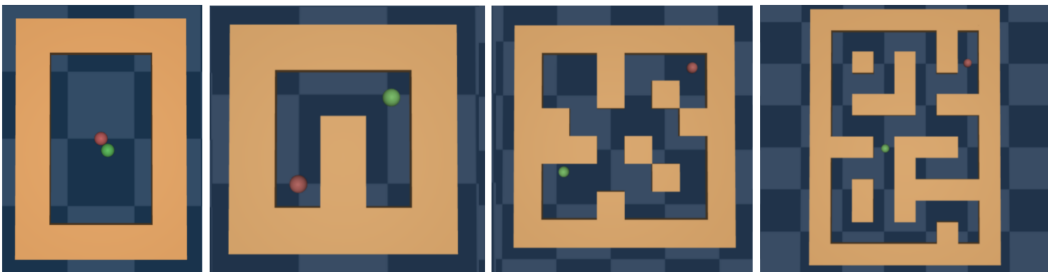


Figure 7: Illustration of Maze2D and AntMaze environments [38].

**AntMaze tasks:** The AntMaze domain extends the Maze2D task by replacing the 2D ball with a more complex 8-DoF "Ant" quadruped robot, presenting a more demanding navigation challenge. This domain is introduced to test the stitching challenge with a morphologically complex robot, better representing real-world robotic navigation tasks. The task uses a sparse 0-1 reward, activated upon reaching the goal. The data is generated by training a goal-reaching policy and using it with the same high-level waypoint generator from maze2d to provide subgoals that guide the agent to the goal. As in Maze2D, the controllers for this task are non-Markovian as they rely on tracking visited waypoints.

## F More Experiments

**Impact of model size.** We investigate the impact of model size on various behavior cloning and decision transformer variants, including BC, DT, ODT, and VDT, under both offline and online

Table 9: The size and the average and standard deviation of the normalized reward in our experiments.

| Dataset                      | Size    | Normalized Reward   |
|------------------------------|---------|---------------------|
| halfcheetah-medium-replay-v2 | 202000  | 27.17 $\pm$ 15.79   |
| hopper-medium-replay-v2      | 402000  | 14.98 $\pm$ 16.32   |
| walker2d-medium-replay-v2    | 302000  | 14.84 $\pm$ 19.48   |
| halfcheetah-medium-v2        | 1000000 | 40.68 $\pm$ 5.12    |
| hopper-medium-v2             | 999906  | 44.32 $\pm$ 12.27   |
| walker2d-medium-v2           | 999995  | 62.09 $\pm$ 23.83   |
| halfcheetah-expert-v2        | 1000000 | 80.30 $\pm$ 35.82   |
| hopper-medium-expert-v2      | 999906  | 100.59 $\pm$ 31.66  |
| walker2d-medium-expert-v2    | 999995  | 112.09 $\pm$ 23.83  |
| pen-human-v1                 | 4800    | 202.69 $\pm$ 154.48 |
| hammer-human-v1              | 10948   | 23.80 $\pm$ 33.36   |
| door-human-v1                | 6504    | 28.35 $\pm$ 13.88   |
| pen-cloned-v1                | 499886  | 108.63 $\pm$ 122.43 |
| hammer-cloned-v1             | 999872  | 8.11 $\pm$ 23.35    |
| door-cloned-v1               | 999939  | 12.29 $\pm$ 18.35   |
| kitchen-complete-v0          | 999800  | 62.25 $\pm$ 19.83   |
| kitchen-partial-v0           | 999800  | 89.49 $\pm$ 14.15   |
| maze2d-umaze-v1              | 999869  | -12.55 $\pm$ 9.82   |
| maze2d-medium-v1             | 1999733 | -3.46 $\pm$ 3.95    |
| antmaze-umaze-v0             | 998573  | 86.14 $\pm$ 34.55   |
| antmaze-medium-diverse-v0    | 999930  | 6.36 $\pm$ 10.07    |
| antmaze-umaze-diverse-v0     | 999000  | 3.48 $\pm$ 18.32    |

settings. As shown in Table 10, performance generally improves with increased model capacity. For example, across all three datasets—halfcheetah, hopper, and walker2d—VDT (online) consistently achieves the best performance for each model size, with scores improving as we move from the smallest configuration (3,1,256) to the largest (12,12,768). The performance saturates or drops slightly on walker2d in the largest model, suggesting that model complexity must be matched with task difficulty and data availability. Similarly, other variants like ODT and DT also benefit from larger models, though the gain is more moderate than VDT. Interestingly, the offline methods also demonstrate strong performance with moderate-size models, especially VDT (offline), which performs competitively or better than its online variant in smaller models. For instance, in the (6,4,256) configuration, VDT (offline) achieves 98.3 on hopper, matching the best result at this size. These results suggest that while increasing model size generally boosts performance, particularly for VDT, the returns diminish and may even reverse if the model becomes too large relative to the dataset, likely due to overfitting or optimisation difficulty in reinforcement learning scenarios.

**Impact of inverse temperature  $\eta$ .** Table 11 shows the impact of the inverse temperature  $\eta$  on policy performance. As  $\eta$  increases from 1 to 3, performance consistently improves, indicating that more substantial advantage weighting helps the model focus on high-value trajectories. In this context,  $\eta$  amplifies the difference between actions, guiding the policy toward more optimal behavior. However, setting  $\eta$  too high (e.g.,  $\eta = 10$ ) leads to performance degradation, likely due to overfitting to a small subset of high-advantage samples and reduced generalization.  $\eta = 3$  achieves the best average performance offline and online. This trend highlights the role of  $\eta$  in controlling the selectivity of the learning process, where a moderate value strikes a good balance between stability and performance.

Table 10: Ablation on the model size. Model size is denoted as  $(x, y, z)$  for number of layers, attention heads, and embedding dimension. **Bold** indicates the best result overall, and underline highlights the best among offline methods.

| Model Size  | Method        | halfcheetah-medium-v2 | hopper-medium-v2 | walker2d-medium-v2 |
|-------------|---------------|-----------------------|------------------|--------------------|
| (3,1,256)   | BC (offline)  | 34.0                  | 44.8             | 72.3               |
|             | DT (offline)  | 42.7                  | 60.3             | 70.6               |
|             | ODT (offline) | 18.3                  | 62.9             | 57.2               |
|             | VDT (offline) | <u>43.6</u>           | <u>98.3</u>      | <u>79.0</u>        |
|             | ODT (online)  | 23.6                  | 70.1             | 52.8               |
|             | VDT (online)  | <b>49.0</b>           | <b>105.9</b>     | <b>89.8</b>        |
| (6,4,256)   | BC (offline)  | 42.6                  | 52.9             | 75.3               |
|             | DT (offline)  | 42.6                  | 67.6             | 74.0               |
|             | ODT (offline) | 42.7                  | 66.9             | 72.2               |
|             | VDT (offline) | <u>43.9</u>           | <u>98.3</u>      | <u>81.6</u>        |
|             | ODT (online)  | 42.2                  | 97.5             | 76.8               |
|             | VDT (online)  | <b>53.5</b>           | <b>108.1</b>     | <b>89.8</b>        |
| (12,12,768) | BC (offline)  | 42.9                  | 67.3             | 69.1               |
|             | DT (offline)  | 39.3                  | 74.9             | <u>75.2</u>        |
|             | ODT (offline) | 42.7                  | 79.1             | 66.0               |
|             | VDT (offline) | <u>44.0</u>           | <u>96.0</u>      | 74.1               |
|             | ODT (online)  | 43.9                  | 99.8             | 82.1               |
|             | VDT (online)  | <b>54.9</b>           | <b>108.9</b>     | <b>84.2</b>        |

Table 11: Ablation on the hyperparameter  $\eta$ .

| Dataset                      | Offline Training |          |          |           | Online Tuning |          |          |           |
|------------------------------|------------------|----------|----------|-----------|---------------|----------|----------|-----------|
|                              | $\eta=1$         | $\eta=3$ | $\eta=5$ | $\eta=10$ | $\eta=1$      | $\eta=3$ | $\eta=5$ | $\eta=10$ |
| halfcheetah-medium-expert-v2 | 34.2             | 93.9     | 88.65    | 59.1      | 77.3          | 101.7    | 10.9     | 103.9     |
| hopper-medium-v2             | 18.3             | 98.3     | 97.6     | 70.0      | 29.6          | 108.1    | 93.1     | 100.3     |
| walker2d-medium-replay-v2    | 65.9             | 82.3     | 82.1     | 46.9      | 58.3          | 95.5     | 96.9     | 22.1      |
| antmaze-umaze-v0             | 50.7             | 100.0    | 90.0     | 88.3      | 39.1          | 110.0    | 110.0    | 75.8      |
| Average                      | 42.3             | 93.6     | 89.1     | 66.1      | 51.1          | 103.8    | 77.7     | 75.5      |

**Impact of RTG alignment.** Table 12 presents the ablation study on RTG alignment during online tuning. Without RTG alignment, VDT performs worse than offline training on certain tasks, indicating that RTG alignment effectively leverages trajectory signals from online interaction by correcting reward guidance. Incorporating RTG alignment consistently improves performance across all tasks. The average score increases from 75.6 to 94.2, indicating a substantial performance gain. In particular, tasks such as halfcheetah-medium-v2 and walker2d-medium-v2 benefit significantly, demonstrating that RTG alignment is especially effective when dealing with suboptimal trajectories.

Table 13: Ablation study on model components during online tuning. All experiments are repeated three times, and the average value is taken.

| Advantage Weighting | Regularization | hopper-medium-v2 | walker2d-medium-expert-v2 | antmaze-umaze-v0 |
|---------------------|----------------|------------------|---------------------------|------------------|
| ✓                   |                | 104.1            | 110.2                     | 90.5             |
|                     | ✓              | 107.0            | 94.3                      | 100.0            |
| ✓                   | ✓              | 108.1            | 112.7                     | 110.0            |

Table 12: Ablation study on RTG alignment. Online Tuning-w/o refers to VDT during online tuning without RTG alignment.

| Datasets                     | Offline Training | Online Tuning-w/o | Online Tuning |
|------------------------------|------------------|-------------------|---------------|
| halfcheetah-medium-replay-v2 | 39.4             | 36.0              | 49.2          |
| hopper-medium-replay-v2      | 96.0             | 99.4              | 119.2         |
| walker2d-medium-replay-v2    | 82.3             | 85.6              | 95.5          |
| halfcheetah-medium-v2        | 43.9             | 11.7              | 53.5          |
| hopper-medium-v2             | 98.3             | 99.6              | 108.1         |
| walker2d-medium-v2           | 81.6             | 44.0              | 89.8          |
| halfcheetah-medium-expert-v2 | 93.9             | 80.6              | 101.7         |
| hopper-medium-expert-v2      | 111.5            | 111.0             | 117.8         |
| walker2d-medium-expert-v2    | 110.4            | 112.3             | 112.7         |
| Average                      | 84.1             | 75.6              | 94.2          |

**Role of different components.** As shown in Table 13, we also conduct an ablation study on advantage weighting and regularization in online fine-tuning for VDT. Since the sampling stage is independent of the training phase, and we have already demonstrated the advantage of value guidance during sampling in Table 3, we do not perform an additional ablation for the sampling process. We observe that the components of VDT exhibit similar effectiveness in the online setting as in the offline one. Using either component individually leads to performance improvement while combining both yields the best results. This demonstrates that value-guided methods are effective in both online and offline scenarios.

## G Broader Impact

The Value-Guided Decision Transformer advances decision-making automation by improving adaptability across offline and online settings, offering potential benefits in areas like robotics, logistics, and personalized AI assistance. While designed to enhance efficiency and scalability, its adoption invites considerations around balancing human-AI collaboration—such as ensuring human oversight in critical decisions and avoiding over-reliance on automated systems. By prioritizing transparency in value-guided objectives and fostering partnerships between developers and domain experts, VDT’s deployment can support human-centric innovation while addressing practical challenges responsibly.